

EXPLORING THE EFFECTS OF DIABETES MELLITUS ON ISOTOPIC RATIOS

by

Alexis Ja'net Baide, B.S.

A thesis submitted to the Graduate Council of  
Texas State University in partial fulfillment  
of the requirements for the degree of  
Master of Arts  
with a Major in Anthropology  
December 2021

Committee Members:

Nicholas P. Herrmann, Chair

Deborah L. Cunningham

Daniel J. Wescott

**COPYRIGHT**

by

Alexis Ja'net Baide

2021

## **FAIR USE AND AUTHOR'S PERMISSION STATEMENT**

### **Fair Use**

This work is protected by the Copyright Laws of the United States (Public Law 94-553, section 107). Consistent with fair use as defined in the Copyright Laws, brief quotations from this material are allowed with proper acknowledgement. Use of this material for financial gain without the author's express written permission is not allowed.

### **Duplication Permission**

As the copyright holder of this work I, Alexis Ja'net Baide, refuse permission to copy in excess of the "Fair Use" exemption without my written permission.

## **DEDICATION**

I dedicate this master's thesis to my mama, Sandra Quesada; you are my rock.

## ACKNOWLEDGEMENTS

This material is based upon work supported by the Grady Early Research Endowment in Forensic Anthropology, the Graduate College Thesis Research Support Fellowship, and the National Science Foundation Graduate Research Fellowship Program under Grant No. (1840989). Any opinions, findings, and conclusions or recommendations expressed in this material are those of the author(s) and do not necessarily reflect the views of the National Science Foundation.

I would like to thank all facilities and staff at Texas State University and the University of Utah who made this research possible. Thank you to all members with the Forensic Anthropology Board at FACTS who reviewed and strengthened my research proposal. Thank you Dr. Joan Brenner-Coltrain, Daniel Dalmas (PhD Student), and staff at SIRFER for processing samples. Thank you, Dr. Cunningham, for your collaboration and receptiveness to a new methodology. Thank you especially to the families and donors with the Willed Body Donation for your contribution to science and to this research.

Furthermore, I would like to thank faculty who mentored me as a student and a scholar. First to my primary advisor, Dr. Herrmann, for joining me on a journey of untreaded territory. Thank you for encouraging me to pursue a topic that brings me passion and excitement. Dr. McKeown, you are a hidden charm to us graduate students. Thank you for your kindness, guidance, and support. Thank you Dr. Kilby for always having an open door when I needed professional advice. Dr. Ahlman, the skills you taught me in research design/development played a huge role in crafting this thesis.

Finally, thank you to this program for introducing me to long-lasting friendships. I thank my best friend, Fatimah, for always understanding me. Megan Veltri, you are a role model to many of us. Thank you to my cohort and the cohorts before and after us for the great memories and tons of laughs.

The COVID-19 pandemic, 2020 presidential election, and powerful political-social movements (e.g., Black Lives Matter, Trans Lives Matter, #MeToo) are some reflections of our recent challenging times. So, thank you all. Tremendously.

## TABLE OF CONTENTS

	<b>Page</b>
ACKNOWLEDGEMENTS .....	v
LIST OF TABLES .....	viii
LIST OF FIGURES .....	ix
LIST OF ABBREVIATIONS .....	x
CHAPTER	
I. INTRODUCTION .....	1
Research Purpose and Hypotheses.....	1
II. BACKGROUND INFORMATION / LITERATURE REVIEW .....	3
Stable Isotopes .....	3
Stable Isotopic Analysis.....	3
Isotopes in Tissue.....	4
Isotopes in Drinking Water.....	5
Isoscapes .....	9
Isotopes and Disease .....	10
III. MATERIALS AND METHODS.....	14
Water Sampling .....	14
Isoscapes .....	14
Human Bone Sampling .....	18
Statistics .....	21
IV. RESULTS .....	23
Tap Water Stable Isotope Analysis.....	23
Isoscapes .....	23
Bone Stable Isotope Analysis .....	29
Statistical Analyses .....	29

V.	DISCUSSION.....	35
	Water Surveys.....	35
	Isoscapes.....	35
	Contributions to Anthropology.....	36
	Apatite $\delta^{18}\text{O}$ .....	37
VI.	FUTURE RESEARCH.....	41
VII.	CONCLUSION.....	43
	APPENDIX SECTION.....	44
	REFERENCES.....	76

## LIST OF TABLES

<b>Table</b>	<b>Page</b>
1. Known medical and residential data of donors sampled with the TXSTDSC.....	19
2. Sampled donors' sex, age, diabetic status, and residency.....	20
3. Average tap water $\delta^{18}\text{O}$ results using data available at waterisotopes.org (WI), thesis data (AJB), and the compiled data together.....	24
4. Results of apatite $\delta^{18}\text{O}$ to n=17 donors .....	29
5. Descriptive statistics of non-diabetics' and diabetics' apatite $\delta^{18}\text{O}$ .....	31
6. Descriptive statistics of apatite $\delta^{18}\text{O}$ to donors from Austin, Texas.....	32
7. Descriptive statistics of apatite $\delta^{18}\text{O}$ values of donors from San Antonio, Texas.....	33

## LIST OF FIGURES

Figure	Page
1. Map of Austin, Texas with yellow markers indicating previously sampled tap water locations ( <a href="http://waterisotopes.org">http://waterisotopes.org</a> ) and blue markers indicating n=20 tap water samples collected by the author as part of this thesis .....	16
2. Map of San Antonio, Texas with yellow markers indicating previously sampled tap water locations ( <a href="http://waterisotopes.org">http://waterisotopes.org</a> ) and blue markers indicating n=30 tap water samples collected by the author as part of this thesis .....	17
3. Superior view of left 6 <sup>th</sup> rib of donor 2013.053 .....	21
4. Texas tap water $\delta^{18}\text{O}$ results clipped to Travis County .....	25
5. Texas tap water $\delta^{18}\text{O}$ results, compiled with thesis data, and clipped to Travis County.....	26
6. Texas tap water $\delta^{18}\text{O}$ results and clipped to Bexar County .....	27
7. Texas tap water $\delta^{18}\text{O}$ results, compiled with thesis data, and clipped to Bexar County.....	28
8. Histogram of apatite d18O ( $\delta^{18}\text{O}$ ) with normality curve .....	30
9. Box plots of non-diabetics' and diabetics' apatite d18O ( $\delta^{18}\text{O}$ ).....	31
10. Box plots comparing apatite $\delta^{18}\text{O}$ values of non-diabetics to diabetics within Austin, Texas (TX) .....	32
11. Box plots comparing apatite $\delta^{18}\text{O}$ values of non-diabetics to diabetics within San Antonio, Texas (TX).....	34

## LIST OF ABBREVIATIONS

<b>Abbreviation</b>	<b>Description</b>
$\delta^{18}\text{O}$	Stable Oxygen Isotope Ratio
$\delta^{15}\text{N}$	Stable Nitrogen Isotope Ratio
$\delta^{13}\text{C}$	Stable Carbon Isotope Ratio
$\delta^2\text{H}$	Stable Hydrogen Isotope Ratio
DM	Diabetes Mellitus
TXSTDSC	Texas State University Donated Skeletal Collection
SIRFER	Stable Isotope Ratio Facility for Environmental Research

## I. INTRODUCTION

An essential role for biological anthropologists is to estimate the biological profile of skeletonized individuals. The biological profile consists of estimating an individual's sex, age at death, stature, and ancestry (Ubelaker, 2019). Further analyses of human skeletal remains may provide indication of trauma and disease to the individual before death if evidence is present. Results of such analyses can be essential in both forensic and archaeological contexts.

### **Research Purpose and Hypotheses**

The absence of pathological evidence on bone is not always indicative of a healthy individual. Not all diseases physically express themselves on bone. The absence of physical expression may also indicate an affected individual with less severe physical symptoms, a later onset of disease, or an individual with a better immune response compared to other individuals affected with the same condition (Wood et al., 1992). Applying stable isotopic analyses to skeletal assessments may help improve the disadvantages of visual analyses. Furthermore, the identification of diseases by isotopic analysis can provide additional discriminative factors to the biological profile and aid in the identification of unknown individuals.

Direct relationships of stable isotopic analysis to human pathology have not been widely conducted due to the lack of human skeletal remains whose health and history are well known (Richards & Montgomery, 2012). I hypothesize that stable oxygen isotope ratios ( $\delta^{18}\text{O}$ ) can be used as an indicator for metabolic disease expressed in human bone apatite. Therefore, I explored the effects of diabetes mellitus (DM) on apatite  $\delta^{18}\text{O}$  using a skeletal collection with known diabetes history. Diabetes mellitus is a metabolic disease

caused from abnormal insulin sensitivity (type II) or can express itself as an autoimmune disease, which results in the inability to produce sufficient insulin for blood sugar transport in the body (type I) (CDC, 2019). Affected individuals experience increased appetite, urination, and water consumption and are at greater risk for blindness, fractures, heart disease, kidney disease, lower-limb amputations, and stroke (CDC, 2019).

I hypothesize that individuals with known diabetes mellitus will have apatite  $\delta^{18}\text{O}$  more like their drinking water, thus significantly lower apatite  $\delta^{18}\text{O}$  compared to individuals with no record of reported DM disease. A null hypothesis will result in no significant difference in isotopic ratios between diabetic individuals and non-diabetic individuals.

This research was accomplished by examining differences in apatite  $\delta^{18}\text{O}$  between a known type II diabetic group and a healthy/control group from the Texas State Donated Skeletal Collection (TXSTDSC). All donors used in this exploratory study were residents of San Antonio, Texas or Austin, Texas area for at least six years prior to death. Studying skeletal collections with known DM will contribute to a better understanding of past human behaviors (Schoeninger and Moore 1992), patterns of disease, and the affected populations themselves. This research is aimed to enhance understanding of disease-influenced variations on stable isotope ratios, which will allow researchers to better interpret existing isotopic data and may provide an additional sector of analysis for skeletal remains.

## II. BACKGROUND INFORMATION / LITERATURE REVIEW

### Stable Isotopes

An isotope represents a form of an element with the same number of protons and the same number of electrons; however, it contains a different number of neutrons to the most abundant form of the element. Since the properties of an atom are driven by the configuration of electrons, all isotope forms of the element will continue to express the same properties (Schoeninger, 2011). However, an isotope's different number of neutrons results in a different mass to the most abundant form of the element. This difference in mass results in a different rate of reaction during chemical processes (Schoeninger, 2011). For example, the stable isotopes of oxygen are  $^{16}\text{O}$ ,  $^{17}\text{O}$ , and  $^{18}\text{O}$ , and molecules of  $^{16}\text{O}$  will react faster in comparison to the molecules in  $^{18}\text{O}$ . Furthermore, differences in mass, and thus reaction rates, can lead to isotope fractionation or isotope discrimination for a heavier or lighter isotope during synthesis and metabolism (Schoeller, 1999). Isotope fractionation can result in a heavier or lighter elemental signature in the body compared to the element's input signature.

### Stable Isotopic Analysis

Isotopes can be stable or radioactive. In this thesis, I will only discuss stable isotopes. Stable isotopes are naturally occurring elements and do not decay over time. Stable isotopic analysis is expressed as the ratio of two stable isotopes. For example, stable oxygen isotopic analysis can be presented as the ratio of  $^{18}\text{O}/^{16}\text{O}$ . Results of stable isotopic analysis are presented as  $\delta$  for delta, or  $\delta$ , due to differences in fractionation during chemical reactions such as transfer from an ocean to the atmosphere (Schoeninger, 2011). Results of isotopic analysis in the form of  $\delta$  consider known fractionation. For

example, stable oxygen isotopic analysis of water is presented as the difference between the ratio of  $^{18}\text{O}/^{16}\text{O}$  in the immediate sample and the standard mean of ocean water (Schoeninger, 2011). The difference is multiplied by 1,000 and the unit of measurement is per mil (‰).

### **Isotopes in Tissue**

The phrase “You are what you eat” has often been used as an analogy for analyzing diet, nutrition, and migration patterns of skeletonized individuals using isotopic ratios (Fuller et al., 2004;2005; Reitsema, 2013). Stable isotope ratios differ among food, water, plant, and animal sources which makes it possible to trace diet, mobility, and locality. For example, water stable oxygen isotope ratios ( $\delta^{18}\text{O}$ ) differ between geographic regions which are reflected in the tissue of residents (Craig, 1961; Longinelli, 1984). However, plasticity, nutritional stressors, isotope fractionation, and metabolic diseases may also influence isotopic ratios (Temple, 2008; Krueger & Sullivan, 1984). Howbeit strontium isotopic ratios do not fractionate when undergoing chemical reactions (Schoeninger, 2011), therefore strontium may be an exception where these effects may not be reflected in the strontium chemistry of tissues. Previous research has demonstrated that chemical signatures preserved in tissue are complex as examples of fasting, weaning, anorexia, bulimia, and starvation have been shown to affect tissue breakdown, fractionation, and isotopic ratios (Hobson et al., 1993; Katzenberg et al., 1996; Petzke et al., 2006).

Stable isotopic chemical signatures are preserved in tissues such as teeth and bone, which enable researchers to assess their abundance within skeletal remains (Sealy, 2001). Since bone continues to remodel throughout life (Buikstra & Ubelaker, 1994),

chemical signatures of food consumed are reflected in tissues up until death.

Bone is composed of compact cortical bone and spongy trabecular bone. Tissues of bone are composed of collagen, or protein, and hydroxyapatite.  $\delta^{18}\text{O}$  can be extracted from hydroxyapatite. Bone hydroxyapatite is often referred to as “bioapatite” or “apatite.” From this point forward, hydroxyapatite will be referred to as apatite. Models have shown that bodily  $\delta^{18}\text{O}$  are most correlated with local drinking water (Longinelli, 1984) and may be influenced by factors such as diet and atmosphere.

### **Isotopes and Drinking Water**

To understand isotopes in tissues it is important to also discuss isotopes in drinking water. The first study to monitor differences in tap water samples across the United States was conducted by Bowen and colleagues in 2007. This study highlighted differences ranging up to 23.6‰ in stable oxygen ratio ( $\delta^{18}\text{O}$ ) and to 163‰ in stable hydrogen isotope ratio ( $\delta^2\text{H}$ ) across greater distances, such as inland to coastal regions. Differences also lie in local regions, albeit on a smaller scale, due to variation in water treatments during the source-to-consumer journey (Bowen et al., 2007). This source of variation will be discussed later when comparing isotopic ratios of local spaces in Austin, Texas which is primarily sourced by the Colorado River and local distributions in San Antonio, Texas where tap water is sourced by four different aquifers.

Results published in 2007 by Bowen and colleagues summarizes  $\delta^{18}\text{O}$  and  $\delta^2\text{H}$  ratios compiled throughout the United States. The authors collected 510 tap water samples from across the states with few gaps greater than about 100km in distance. In addition, 568 tap water samples were collected from 22 cities in the US and the province of Alberta as part of a monthly data collection effort (Bowen et al., 2007). Descriptive

results of the monthly survey were not statistically different to the descriptive statistics of the US spatial data set. Temporal or monthly variability was only able to be assessed locally as tap water samples collected to interpolate the spatial distribution across the US were not ascribed to a particular temporal period or gathered during a singular month of the year (e.g., January). Local temporal variability was low relative to overall spatial variability. This also implies the spatial distribution of  $\delta^{18}\text{O}$  and  $\delta^2\text{H}$  interpolation map across the US is not temporally tethered, thus one cannot be certain how close the sampled tap water reflects the true mean of the annual variability for any given city. Bowen et al. (2007) recommend sampling over a greater time span than one year to obtain a more representative survey of temporal tap water variability. The authors conclude that temporal variability is low in most regions, or a tap water sample collected at random would be like the average tap water  $\delta^{18}\text{O}$  and  $\delta^2\text{H}$  ratios for the region (Bowen et al., 2007). The authors note the interpolated spatial distribution of  $\delta^{18}\text{O}$  and  $\delta^2\text{H}$  may be biased as 63% of tap water samples were collected during December 2002 and March 2003.

The construction of isoscapes has created new opportunities and methodologies in archaeological and forensic contexts. A more recent development is the use of water signatures across the US to trace migratory animals (Cerling et al., 2006). Stable  $\delta^{18}\text{O}$  and  $\delta^2\text{H}$  isotopic signatures of precipitation water has shown to differ across regions based on elevation, latitude, and climate (Bowen & Revenaugh, 2003), therefore these patterns can then be used to detect regions of origin by  $\delta^{18}\text{O}$  and  $\delta^2\text{H}$  signatures found in hair, nail, and feathers (Podlesak et al., 2012).

Ehleringer and colleagues (2008) developed a model to estimate geographic

origin by use of oxygen isotope ratios found in human hair.  $\delta^{18}\text{O}$  obtained from human hair were correlated with geography by least-squares regression analysis. Statistical models were developed to predict bodily  $\delta^{18}\text{O}$  and  $\delta^2\text{H}$  ratios in humans based on the reactions and factors which affect water input and water output. Modeling results were then tested by an additional random hair survey obtained from a barber shop. The random hair survey consisted of 65 hair samples. The authors predicted 85% samples'  $\delta^2\text{H}$  and 86% samples'  $\delta^{18}\text{O}$  values accurately when compared to the model-prediction values (Ehleringer et al., 2008). The authors note the hair prediction model values show heaviest  $\delta^{18}\text{O}$  ratios to be exhibited along the Gulf Coast states and Central Texas area.

Prediction maps show bodily water pool, or the water in human tissues (e.g., hair, nails, bones), to be most influenced by local drinking water. Ehleringer and colleagues (2008) note the majority of fluid intake by water, juices and milks are derived by local tap water sources. Although bodily water is most heavily influenced by tap water, it is also influenced by other factors such as diet intake and atmospheric oxygen. The authors used a "near constancy" value to take account for dietary intake values in the prediction formulae, noting most foods are derived from the continental food market opposed to solely consuming locally derived foods. The developed prediction models adjust slopes to the degree of diet makeup and contribution of continental foods and local goods (Ehleringer et al., 2008). Ehleringer and colleagues (2008) highlight that the prediction of hair  $\delta^2\text{H}$  values might be affected by low-protein diets, however, low-protein diets are not expected to affect hair  $\delta^{18}\text{O}$  prediction values. The authors recommend future research to explore potential influencing factors by examining hair of individuals with diseases or disorders such as bulimia and anorexia. Together, the model prediction models of hair

$\delta^{18}\text{O}$  and  $\delta^2\text{H}$  signatures, known hair growth rates, and tissue turnover rates provide parameters to estimate locality movement and timing of movement in humans.

An expansion of these models was presented by Podlesak et al. (2012) to develop a prediction model for  $\delta^2\text{H}$  and  $\delta^{18}\text{O}$  bodily values in humans presented by mass balance. The study identified migratory behavior and the rate of equilibrium to identify residents from non-locals. Podlesak and colleagues (2012) considered all sources affecting bodily water such as drinking water, water and hydrogen-oxygen molecules in foods consumed, atmospheric dioxygen, and atmospheric water vapor. To account for equilibrium status, water output in the forms of urine, sweat, fecal water, water vapor loss, and carbon dioxide loss were accounted for in the mass balance equations. Mass balance models were developed for the adult male and adult female following the Kohn (1996) animal model. Signatures of  $\delta^2\text{H}$  and  $\delta^{18}\text{O}$  in foods were held constant for modeling predictions to reflect the average American diet, which consists of global foods. Podlesak and colleagues (2012) then compared predicted body water models of a resident from Houston traveling to Salt Lake City, UT or Chicago, IL and tracked the rate in days for the traveler to be indistinguishable from residents. Results indicated a visitor to Chicago had similar isotopic bodily signatures to Chicago residents after 14-18 days from arrival and a visitor to Salt Lake City expressed similar bodily signatures to residents after 25-32 days from arrival. Podlesak et al. (2012) attribute these differences in half-lives to the greater difference in isotopic ratios of Salt Lake City to Houston than Chicago to Houston, thus requiring more time for a visitor to Salt Lake City to reach equilibrium with residents. Podlesak et al. (2012) emphasize the applicability of bodily prediction models to identify non-residents or visitors of an area within a narrow time frame. The

body water prediction models are useful to identify movement of persons between areas with different  $\delta^{18}\text{O}$  and  $\delta^2\text{H}$  isotopic signatures within a 1-week period, whereas hair signatures reflect monthly changes. The authors note bodily water can be sampled by surveying blood, urine, or breath. Moreover, other body tissues such as bones and teeth may also be modeled to detect human migratory patterns as these sources are also influenced by bodily water (Podlesak et al., 2012).

### **Isoscapes**

Environmental data such as drinking water can be visually presented as isoscapes, which can be created in ArcGIS. ArcGIS is a geographic information system (GIS) maintained by Esri and it allows users to visualize geographical statistics. For example, data in Bowen et al. (2007) are presented in the form of isoscapes. Isoscapes consist of mapping known data, such as tap water  $\delta^{18}\text{O}$ , and applying a prediction model which accounts for latitude, longitude, and the spatial weight of distance between known data points using functions in ArcGIS Pro 2.5.0. This results in a continuous gradient-like representation of estimated tap water  $\delta^{18}\text{O}$  for a region based on surrounding known data. These models are often used by archaeologists and anthropologists to estimate the region of origin of their sample at hand (West et al., 2008). In forensic anthropology,  $\delta^{18}\text{O}$  isoscapes are more often used to estimate the region of origin of unknown individuals. The method enables researchers to omit regions which do not reflect the chemical signatures of the sample and to then narrow down possible regions which do reflect a similar chemical signature and thus where the unknown individual could originate (Ehleringer et al., 2008).

## Isotopes and Disease

Previous research has been conducted on the physiological effects of disease on isotopic ratios. This perspective has not been fully explored as pathological specimens are typically avoided for destructive analyses. This begs the question how scientists may explore directly related pathological variations in isotopic ratios, especially if the skeletal remains do not exhibit physical evidence of underlying disease. Areas on bone with physical lesions have shown to exhibit intraskeletal variation in stable carbon isotope ratio ( $\delta^{13}\text{C}$ ) and stable nitrogen isotope ratio ( $\delta^{15}\text{N}$ ) (Olsen et al., 2014). When comparing intraskeletal composition of samples with various metabolic conditions to the “normal,” or non-pathological bone, Olsen and colleagues (2014) found significant differences within degenerative joint lesions, osteomyelitis lesions, and areas of fracture trauma to the bone. These differences are attributed to negative nitrogen balances indicated by a  $\delta^{15}\text{N}$  enrichment due to changes in protein metabolism during infection and healing (Olsen et al., 2014; Katzenberg & Lovell, 1999). The interpretation of  $\delta^{15}\text{N}$  balances has been studied since the first discovery of  $\delta^{15}\text{N}$  enrichment caused by starvation in birds (Hobson et al., 1993). These studies may be useful when recommending limitations of sample procurement from pathological bone, but the expression of bone pathology may vary based on severity, biological plasticity, and disease type.

Furthermore, these studies enable researchers to better understand how tissues function within the body. Samples taken from individuals with underlying conditions affecting the entire body such as rickets or AIDS reveal lower differences between regions of affected bone and “normal” bone suggesting newly formed tissues may also reflect the individuals’ current diet (Olsen et al., 2014; Katzenberg & Lovell, 1999).

Katzenberg and Lovell's (1999) research of intraskeletal composition from individuals with known medical histories also highlights the potential differences in isotopic variations when etiology is in question. For this reason, it may be best for a multi-isotopic approach to be applied when interpreting the life history of archaeological or unknown remains by use of isotopic analysis.

Specific to metabolic conditions are studies focused on the use of  $\delta^{15}\text{N}$  to assess catabolic stress. Generally, stable isotopes are a form of an element, e.g.,  $^{16}\text{O}$  with a different number of neutrons creating a compound with a different weight, e.g.,  $^{18}\text{O}$ . These differences in weight are critical in understanding fractionation processes within the body. Chemical reactions during digestion or metabolism may be biased towards an isotope based on its weight. Theoretically, these fractionation processes can be modeled (Schoeller, 1999). Not surprisingly, the human system is far more complex than a singular metabolic route under homeostasis. Further exploration of direct metabolic relationships with stable isotopes can help scientists create models of known pathways and etiology. Hatch and colleagues (2006) first identified the potential use of stable isotopes to identify eating disorders. Isotopic analyses were conducted on hair samples of patients diagnosed with anorexia, bulimia, anorexia and bulimia, and control healthy participants. Results of  $\delta^{15}\text{N}$  and  $\delta^{13}\text{C}$  were significantly different from control groups and isotopic ratios of individuals with bulimia were statistically different from the control depending on the segment of hair shaft sampled (Hatch et al., 2006).

Anorexia is the fear of weight gain resulting in reduction of calories consumed and weight loss. Bulimia is categorized as cycles of bingeing and purging resulting in irregular eating habits and fluctuating weight. As mentioned above, it has previously been

observed that starvation can lead to nitrogen enriched isotope ratios in bird bones (Hobsen et al., 1993). When an individual is under stress and protein-deprived resulting in weight loss, the body consumes its own energy, and these tissues result in a higher trophic level. The elevated  $\delta^{15}\text{N}$  signatures may be stored in recycled tissues used during growth, development, and remodeling (Hatch et al., 2006). These fluctuating periods of stress and starvation may be reflected differently in hair segments depending on the time interval reflected in old and new hair growth to the severity of the disorder at the time of growth. This study plays an important role for understanding variation between an individual with different  $\delta^{15}\text{N}$  values in comparison to a larger sample which they cohabitate.

Similarly, Reitsema and Crews (2011) have revealed significantly lower  $\delta^{18}\text{O}$  stable isotope ratios in bone collagen of mice with sickle-cell disease to healthy mice. The sickest mice expressed the lowest  $\delta^{18}\text{O}$  ratios. This study was unique as the diet of mice and water source were kept constant throughout the sample. Fractionation levels have been shown to be influenced by respiration, exercise, and smoking (Epstein & Zeiri, 1988; Widory, 2004). These results may be attributed to lesser activity conducted by the sick mice resulting in higher fractionation processes compared to more active, healthy mice (Reitsema and Crews, 2011). However, the authors recommend a better understanding of the etiology to anemia disorders and sickle-cell disease before relating the observed trend to a specific pathology. This study reveals the possibility for the use of  $\delta^{18}\text{O}$  stable isotopes as biomarkers for disease.

Researchers have implicated the possibility of other metabolic diseases to influence isotopic ratios. In 2010, O'Grady and colleagues examined the stable  $\delta^{18}\text{O}$  and

$\delta^2\text{H}$  ratios of mice urea before and throughout streptozotocin-induced diabetes mellitus. Methods were designed to replicate the water fluxes experienced when an individual is insulin-dependent (e.g., Type 1 diabetics). Diabetic-induced mice were not treated throughout the course of the experiment. By week one,  $\delta^{18}\text{O}$  and  $\delta^2\text{H}$  ratios of diabetic mice urine were significantly lower than the control mice. Isotopic ratios of diabetic mice's urea were similar to ratios of drinking water by week four (O'Grady et al., 2010). Usually, isotopic ratios of bodily water are much higher to drinking water due to oxidation and chemical processes undergone during food ingestion (O'Grady et al., 2010). This study reveals the potential of untreated diabetes or irregular insulin treatments among diabetics to result in hyperglycemia, which increases water flux and potentially is recorded isotopically. Although this study mimics conditions of insulin dependent or type I diabetes mellitus, similar symptoms of dehydration and increased urination are also observed among type II diabetes mellitus with gradual expression. Intuitively, a gradual expression of symptoms observed among type II diabetes mellitus may result in longer periods of water flux due to prolonged diagnosis.

Researchers have expressed the potential use of stable isotopes to detect disease, however, finding direct-pathological-induced variations in isotopic ratios is challenging without the ability to control diet, activity levels, or stress in unknown populations. Data and methods from this thesis may help to bridge this gap with the use of donors with known medical histories. This research may also allow researchers to interpret studies of intra-population variability (D'Angela & Longinelli, 1990) when assessing mobility and dietary patterns by use of isotopic ratios.

### III. MATERIALS AND METHODS

#### Water Sampling

All donors analyzed for this thesis are residents of Austin, Texas or San Antonio, Texas, therefore water sampling methods focused on these two cities. A total of 22 water samples were collected from Austin, Texas. The water samples were collected by the author using 4-mL vials (VWR part 66011-526) and labeled 1-22. Water samples were secured with Styrofoam, placed in a lunch box with dry ice, and shipped overnight to the Stable Isotope Ratio Facility for Environmental Research (SIRFER) at the University of Utah for tap water stable oxygen isotope ratio ( $\delta^{18}\text{O}$ ) analysis. Vial #6 was used to collect water from a pond and Vial #18 was used to collect water from Lake Austin by an access point at Redbud Trail. Vials #6 and #18 were removed from statistical analyses as they do not reflect local tap water. The removal of these two vials results in a total of 20 tap water samples collected from Austin, Texas and are indicated by blue markers in Figure 1.

Identical methodology was followed to survey San Antonio, Texas tap water. A total of 30 4-mL tap water samples were collected from San Antonio, Texas. The tap water samples obtained from San Antonio, Texas were labeled in Vials #23 through #52 and shipped overnight to the SIRFER at the University of Utah for stable oxygen isotope analysis. Water samples collected by the author from San Antonio, Texas are indicated by blue markers in Figure 2.

#### Isoscapes

All spatial analysis used to create isoscapes in this thesis follow methods in Bowen et al. (2007). To summarize, these methods consist of using grids in Albers equal area projection, deriving weights between data points from squared inverse Euclidean

distances, and ordinary kriging of the raw data (Spatial Statistics Box, ArcGIS Pro). The krig spatial analyst tool in ArcGIS uses the expected value to observed value and weighs the error by spatial distance. Additionally, ordinary kriging is performed using the spherical semivariogram function in ArcGIS Pro (Bowen et al., 2007).

To create more accurate isoscapes of tap water  $\delta^{18}\text{O}$  for Austin, Texas and San Antonio, Texas, data collected by other researchers and curated at waterisotopes.org were combined with the data of this thesis. Results of 34 tap water samples collected in Austin, Texas are currently curated at waterisotopes.org and reflect an average tap water  $\delta^{18}\text{O}$  of -2.21527‰. The locations and results of tap water samples from Austin, Texas currently available waterisotopes.org are shown as yellow markers in Figure 1 and summarized in Appendix A. Results to eight tap water samples collected in San Antonio, Texas and curated at waterisotopes.org reflect a tap water  $\delta^{18}\text{O}$  mean of -3.84305‰ and are indicated by yellow markers in Figure 2 and data are summarized in Appendix A.



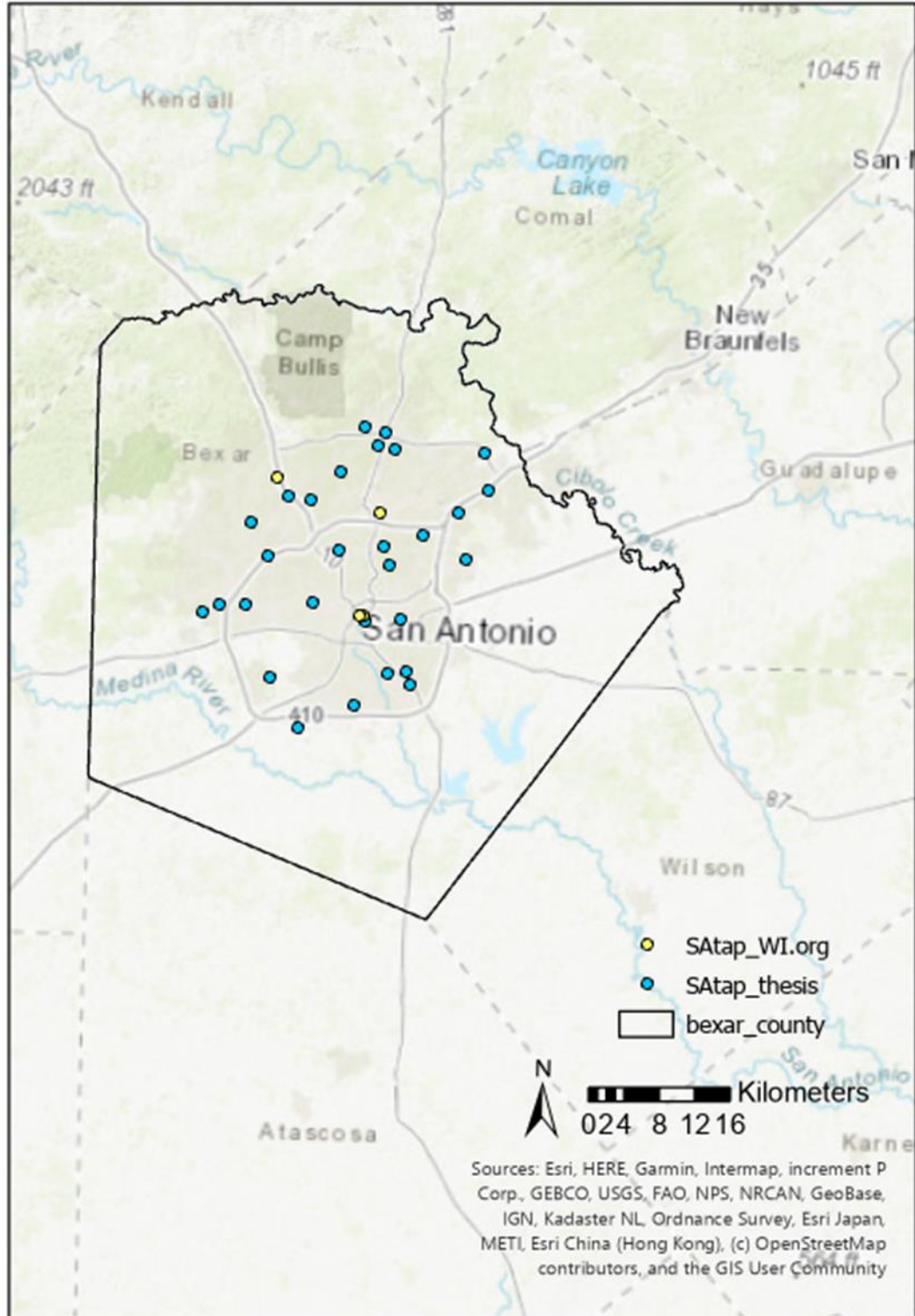


**Figure 2.** Map of San Antonio, Texas with yellow markers indicating previously sampled tap water locations (<http://waterisotopes.org>) and blue markers indicating n=30 tap water samples collected by the author as part of this thesis.

A search query following: Country=US, State/Province=TX, Type=Tap at [https://wateriso.utah.edu/waterisotopes/pages/spatial\\_db/SPATIAL\\_DB.html](https://wateriso.utah.edu/waterisotopes/pages/spatial_db/SPATIAL_DB.html) is summarized in Appendix B. Repetitive locations with identical longitudinal and latitudinal coordinates conducted under the same “Project ID” were averaged to avoid kriging effects during the generation of tap water isoscapes. Averaged results are summarized in Appendix C and were used to create an isoscape of Texas tap water  $\delta^{18}\text{O}$ . For the purposes of this thesis, tap water of Austin, Texas and San Antonio, Texas residents is of interest, therefore, isoscapes were cropped to Travis County (Austin, Texas) and Bexar County lines (San Antonio, Texas) accessible at DOI (2014). Data listed in Appendix C were then compiled with data results from this thesis and identical methods were followed to generate new isoscapes of Travis County and Bexar County.

### **Human Bone Sampling**

A total of 17 donors from the Texas State Donated Skeletal Collection (TXSTDSC) were sampled for apatite  $\delta^{18}\text{O}$  analysis (Table 1). The TXSTDSC consists of donors with known demographics, medical history, and residential histories. An overview of residential data from donors sampled is summarized in Table 1. Age, ethnicity, diabetic status, residential history, sampling history, and sex were used as discriminative factors for donor selection. To assess whether diabetics differ in apatite  $\delta^{18}\text{O}$  to non-diabetics, donors were first selected based on mutual drinking water source and close spatial proximity to one another. The high number of donors local to San Marcos, Texas, enabled centralization of donors to Austin, TX and San Antonio, Texas. Donors were then discriminated to a 6-year minimum occupancy for last known residence. Since bone has a slower turnover rate compared to hair or nails, it was preferred for donors in the sample to reflect long residency.

A longer period as a resident increases the likelihood of drinking water  $\delta^{18}\text{O}$  to be reflected in bone tissue. In addition to having a significant residential history and known medical history, non-diabetics or “control” individuals are also of the same sex, ethnicity, and within +/-10 years of age to the corresponding diabetic individual (Table 2).

**Table 1.** Known medical and residential data of donors sampled with the TXSTDSC.

<b>Donor ID</b>	<b>Last Known Residence</b>	<b>Duration at Last Known Residence (Total Years)</b>	<b>Diabetes (y/n)</b>	<b>Period of Onset (years) if applicable</b>
2009.010	Austin, TX	1985 - 2009 (24)	No	
2010.013	San Antonio, TX	1993 - 2010 (17)	Yes	Unknown
2012.006	Austin, TX	1974 - 2012 (38)	No	
2013.004	San Antonio, TX	1993 - 2013 (20)	No	
2013.014	Austin, TX	1999 - 2013 (14)	Yes	4
2013.037	Austin, TX	1949 - 2013 (64)	No	
2013.053	Austin, TX	1991 - 2013 (22)	No	
2014.007	San Antonio, TX	1993 - 2014 (21)	Yes	11
2014.032	San Antonio, TX	1982 - 2014 (32)	No	
2014.062	Austin, TX	2008 - 2014 (6)	Yes	20
2015.004	San Antonio, TX	2005 - 2015 (10)	Yes	10
2015.023	San Antonio, TX	2009 - 2015 (6)	No	
2015.034	Austin, TX	1970 - 2015 (45)	No	
2015.058	Austin, TX	2005 - 2015 (10)	No	
2015.059	Austin, TX	2005 - 2015 (10)	No	
2016.038	Austin, TX	1960 - 2016 (56)	Yes	2
2017.025	San Antonio, TX	1979 - 2017 (38)	No	

**Table 2.** Sampled donors’ sex, age, diabetic status, and residency. All are self-reported as American White. Known diabetics are denoted by “(D).” Donors are grouped by spatial proximity.

<b>Austin</b>	<b>San Antonio</b>
<u>Group 1: Male (58, 64, 65, 54):</u> 2013.014 (D) 2013.037 2013.053 2015.058	<u>Group 4: Female (78, 69, 80, 79):</u> 2015.004 (D) 2014.032 2017.025 2014.007 (D)
<u>Group 2: Male (53, 58, 54):</u> 2014.062 (D) 2012.006 2015.059	<u>Group 5: Male (70, 79, 70,):</u> 2010.013 (D) 2013.004 2015.023
<u>Group 3: Female (89, 76, 79):</u> 2016.038 (D) 2009.010 2015.034	

Approval for destructive analyses was granted by the Forensic Anthropology Center at Texas State University Board. To minimize destructive analyses, sampling was only performed on elements sampled during a previous NSF-funded project for histological analysis. The left sixth rib was sampled for isotopic analysis in all cases except for donor 2013.037 where the left fourth rib was sampled. A one-inch cross section (Figure 3) from the existing histological cut on the proximal half of the pre-sampled rib was procured under a fume hood using a Dremel rotary tool. Interchangeable Dremel reinforced cutting discs were used between each bone sample to preserve quality control and reduce contamination. Collagen extraction and sample preparation was supervised by Dr. Brenner-Coltrain of the Anthropology Department at the University of Utah. Prepped samples were then transferred to the Stable Isotope Ratio Facility for Environmental Research (SIRFER) at the University of Utah for stable oxygen isotope ratio ( $\delta^{18}\text{O}$ ) analysis.



**Figure 3.** Superior view of left 6<sup>th</sup> rib of donor 2013.053. The rib was previously sampled at mid-shaft for histological analysis. The one-inch bone segment is shown centered and was procured from the proximal or posterior end of the previously cut shaft.

### Statistics

All bone data collected as part of this thesis were tested for normality prior to statistical analyses using IBM SPSS Statistics 26 software. Results of apatite  $\delta^{18}\text{O}$  analysis were tested for the assumption of normality by visual inspection of histograms and one sample Kolmogorov-Smirnov (K-S) tests (Madrigal, 2012). If subsamples are fewer than five, tests for normality were conducted by Shapiro-Wilk (S-W) statistical tests. Where data are normal, boxplots and independent sample t-tests were used to test for statistical differences in sample means (e.g., diabetics' mean apatite  $\delta^{18}\text{O}$  to non-diabetics' mean apatite  $\delta^{18}\text{O}$ ) (Madrigal, 2012).

An independent sample t-test is often used to determine if the average of two samples differ significantly. The test is applicable to two variables: a continuous dependent variable and an independent variable as a category label or string data. For the data in this thesis, diabetic status (independent variable) is string data and apatite  $\delta^{18}\text{O}$  (dependent data) is continuous scale data. The assumptions of an independent sample t-test are random sampling, independence of variance, normality of data, and homoscedasticity. The independence of variance is tested when an independent sample t-test is conducted by an automatic Levene's test. Normality of data are suggested to be tested by K-S and S-W tests. Finally, homoscedasticity suggests that if the null hypothesis is true; the two samples tested are derived from the same population, then variances should be equal (Madrigal, 2012). If the Levene's test is significant then equal variances are not assumed, and SPSS will determine a significance value for the difference of two means where unequal variances are assumed.

## IV. RESULTS

### Tap Water Stable Isotope Analysis

The results of stable oxygen isotopic analysis in water in vials 1-22 are summarized in Appendix D. Vials 1-22 consist of all water collected from Austin, Texas. Note vials number 6 and number 18 do not reflect tap water. Data reflecting Austin, Texas tap water stable oxygen isotope ratio ( $\delta^{18}\text{O}$ ) results range from -1.3 to -0.5 with a mean of -1.116 and standard deviation 0.1693. The results of tap water collected from San Antonio, Texas are summarized in Appendix D (vials 23-52). San Antonio tap water  $\delta^{18}\text{O}$  values range from -5.1 to 0.5 with a mean of -4.120 and standard deviation 0.9604. Vial 27 reflects a tap  $\delta^{18}\text{O}$  of 0.5‰. This value was visually observed as a significant outlier by boxplots and was removed from the dataset. Results discussed throughout the rest of this thesis omit vial 27. The revised tap water  $\delta^{18}\text{O}$  from San Antonio, Texas reflects a mean of -4.279 and standard deviation of 0.4083. The raw tap water  $\delta^{18}\text{O}$  surveyed from Austin, Texas and San Antonio, Texas reveals an average difference of about 3‰.

### Isoscapes

Methods in Bowen et al. (2007) were followed to create an isoscape of Travis County's tap water results (Figure 4) and the updated tap water with the addition of results from this thesis (Figure 5). Isoscapes were created on available tap water  $\delta^{18}\text{O}$  for Bexar County (Figure 6) and with the addition of data in this thesis (Figure 7). Summarized tap water  $\delta^{18}\text{O}$  are listed in Table 3 to reflect the mean of tap water  $\delta^{18}\text{O}$  data currently available (WI) and averages with the addition of thesis data (AJB). As previously mentioned, any data with identical latitude and longitudinal coordinate under

the same project ID were first averaged to reflect an average tap  $\delta^{18}\text{O}$  of the area.

**Table 3.** Average tap water  $\delta^{18}\text{O}$  results using data available at waterisotopes.org (WI), thesis data (AJB), and the compiled data together.

<b>Data</b>	<b>Tap Water <math>\delta^{18}\text{O}</math> (‰) Mean – Averaged</b>	<b>Tap Water <math>\delta^{18}\text{O}</math> (‰) Mean - Kriged</b>
Austin AJB (thesis)	-1.116	-1.115
Austin WI	-2.191	-2.164
Austin Compiled	-1.394	-1.477
SA AJB (thesis)	-4.279	-4.243
SA WI	-4.011	-4.011
SA Compiled	-4.246	-4.226

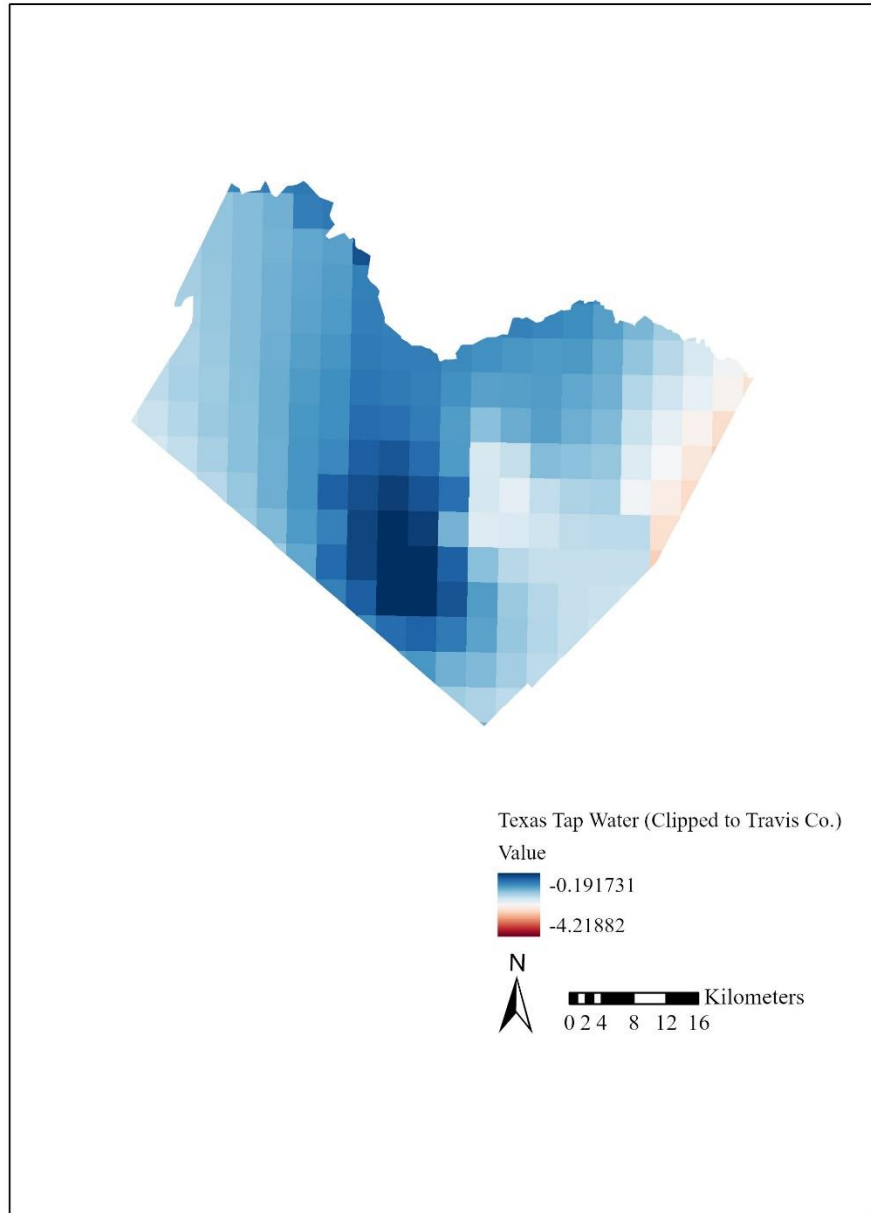


**Figure 4.** Texas tap water  $\delta^{18}\text{O}$  results clipped to Travis County. Symbology is a continuous red-blue color scheme.

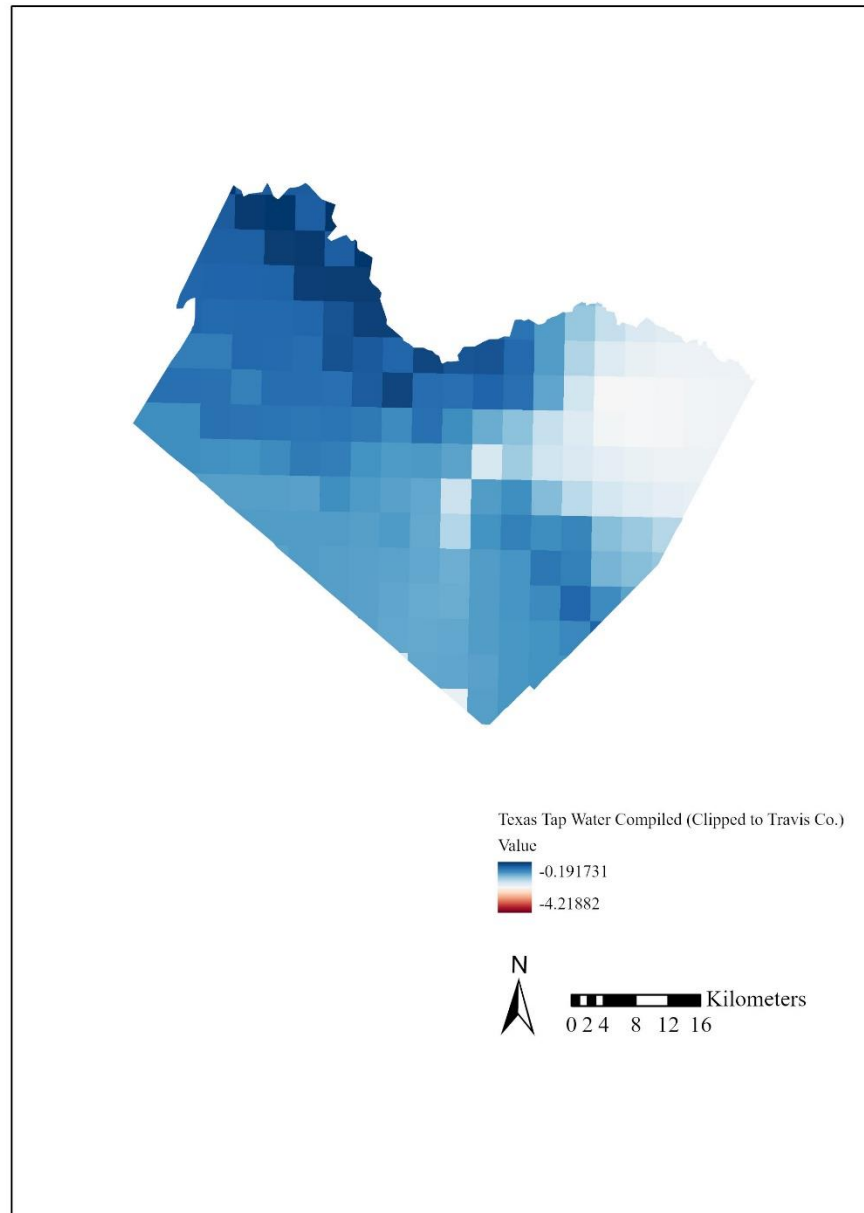


**Figure 5.** Texas tap water  $\delta^{18}\text{O}$  results, compiled with thesis data, and clipped to Travis County. Symbology follows a continuous red-blue color scheme.

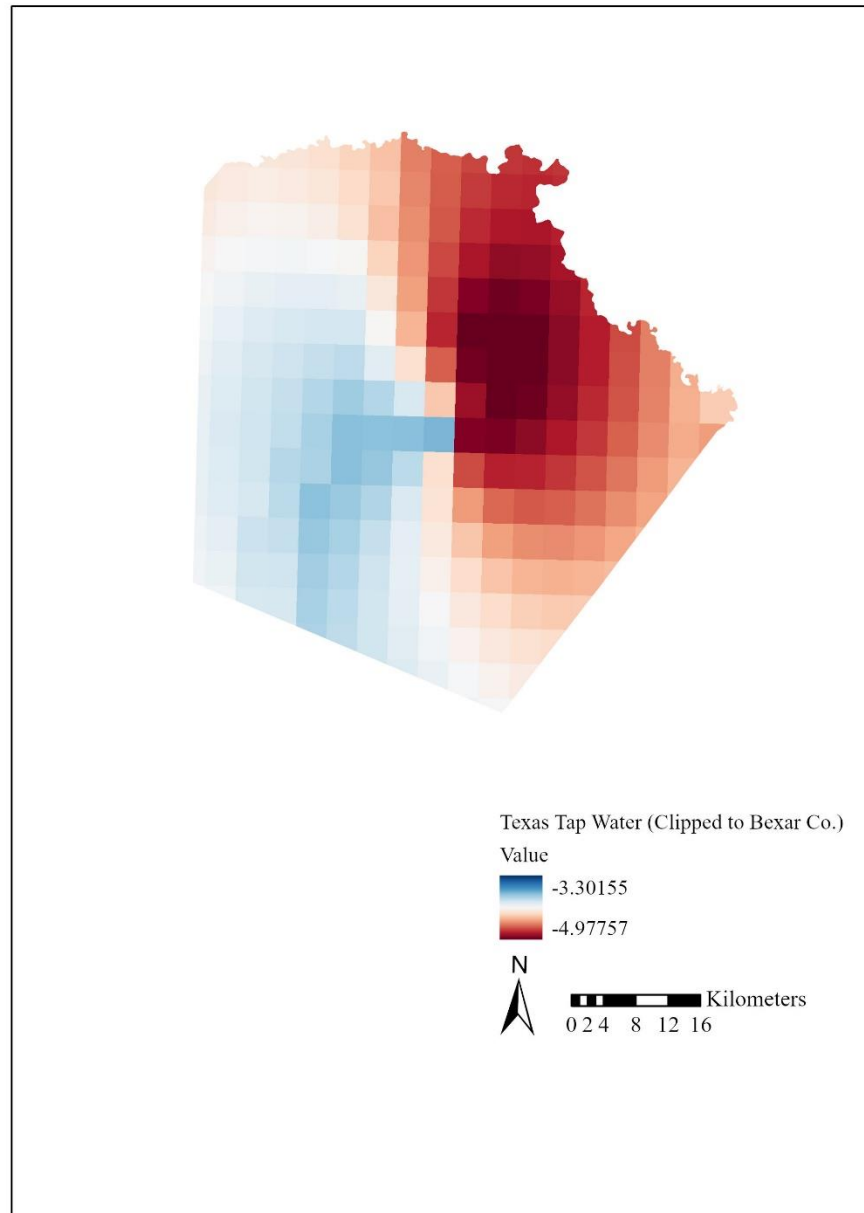


**Figure 6.** Texas tap water  $\delta^{18}\text{O}$  results and clipped to Bexar County. Symbology follows a continuous red-blue color scheme.

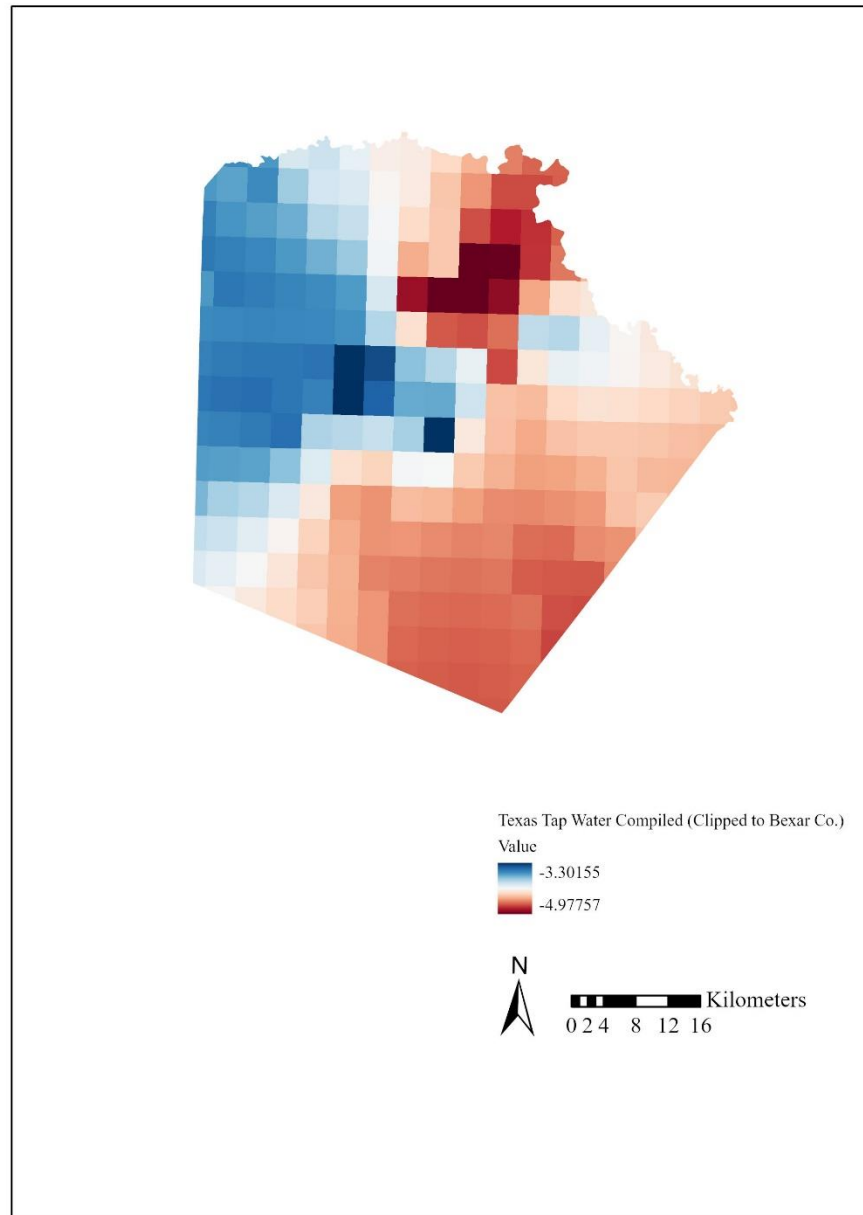


**Figure 7.** Texas tap water  $\delta^{18}\text{O}$  results, compiled with thesis data, and clipped to Bexar County. Symbology follows a continuous red-blue color scheme.

## Bone Stable Isotope Analysis

The result of stable oxygen isotope analysis on bone apatite for 17 rib samples are summarized in Table 4 along with their diabetic status and city of residence. The donors' apatite  $\delta^{18}\text{O}$  range from -4.1 to -1.0 to with a mean of -1.9 and standard deviation 0.1. The standard uncertainty for apatite  $\delta^{18}\text{O}$  is 0.2‰.

**Table 4.** Results of apatite  $\delta^{18}\text{O}$  to n=17 donors.

<b>Donor ID</b>	<b>Residence</b>	<b>Diabetic Status</b>	<b><math>\delta^{18}\text{O}_{\text{VPDB}} (\text{‰})</math></b>
2009.010	Austin, Texas	Non-diabetic	-2.60
2010.013	San Antonio, Texas	Diabetic	-2.30
2012.006	Austin, Texas	Non-diabetic	-2.90
2013.004	San Antonio, Texas	Non-diabetic	-1.60
2013.014	Austin, Texas	Diabetic	-3.60
2013.037	Austin, Texas	Non-diabetic	-2.00
2013.053	Austin, Texas	Non-diabetic	-1.60
2014.007	San Antonio, Texas	Diabetic	-4.10
2014.032	San Antonio, Texas	Non-diabetic	-2.60
2014.062	Austin, Texas	Diabetic	-1.30
2015.004	San Antonio, Texas	Diabetic	-2.20
2015.023	San Antonio, Texas	Non-diabetic	-1.80
2015.034	Austin, Texas	Non-diabetic	-1.00
2015.058	Austin, Texas	Non-diabetic	-2.20
2015.059	Austin, Texas	Non-diabetic	-3.10
2016.038	Austin, Texas	Diabetic	-1.70
2017.025	San Antonio, Texas	Non-diabetic	-2.00

## Statistical Analyses

Apatite  $\delta^{18}\text{O}$  were tested for the assumption of normality by visualization of histograms, which revealed the median is greater than the mean and data are skewed to the left (Figure 8), but a one sample K-S test revealed that apatite  $\delta^{18}\text{O}$  are normally distributed ( $p = 0.200$ ). Visual inspection of histograms and one sample K-S test showed that the sub samples of apatite  $\delta^{18}\text{O}$  to diabetics ( $n = 6$ , mean = -2.533, SD = 1.09,  $p =$

0.200) and non-diabetics ( $n = 11$ , mean =  $-2.127$ , SD =  $0.629$ ,  $p = 0.200$ ) are normally distributed. Since the apatite  $\delta^{18}\text{O}$  sample data are normal, independent t-tests were conducted to assess differences within the sample. To test if diabetics' average apatite  $\delta^{18}\text{O}$  are different to non-diabetics' average apatite  $\delta^{18}\text{O}$ , an independent t-test and visual inspection of boxplots were performed (Table 5; Figure 9). The independent sample t-test revealed there is no difference between the mean of diabetics'  $\delta^{18}\text{O}$  and the mean of non-diabetics' apatite  $\delta^{18}\text{O}$  ( $p = 0.092$ ,  $t = 0.983$ ,  $df = 15$ ). Levene's test indicated equal variances ( $F = 3.236$ ,  $p = 0.092$ ).

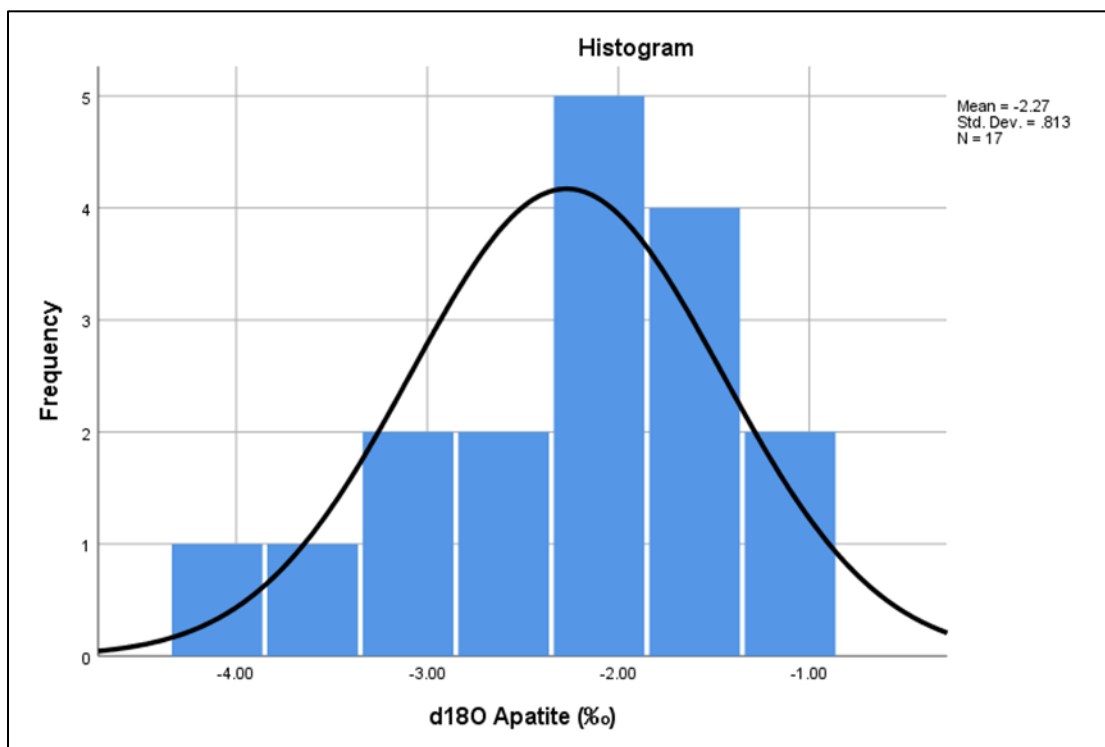


**Figure 8.** Histogram of apatite d18O ( $\delta^{18}\text{O}$ ) with normality curve.

**Table 5.** Descriptive statistics of non-diabetics' and diabetics' apatite  $\delta^{18}\text{O}$ .

	Diabetic Status	N	Mean	Std. Deviation	Std. Error Mean
$\delta^{18}\text{O}$ Apatite	Non-diabetic	11	-2.1273	0.62943	0.18978
	Diabetic	6	-2.5333	1.09301	0.44622

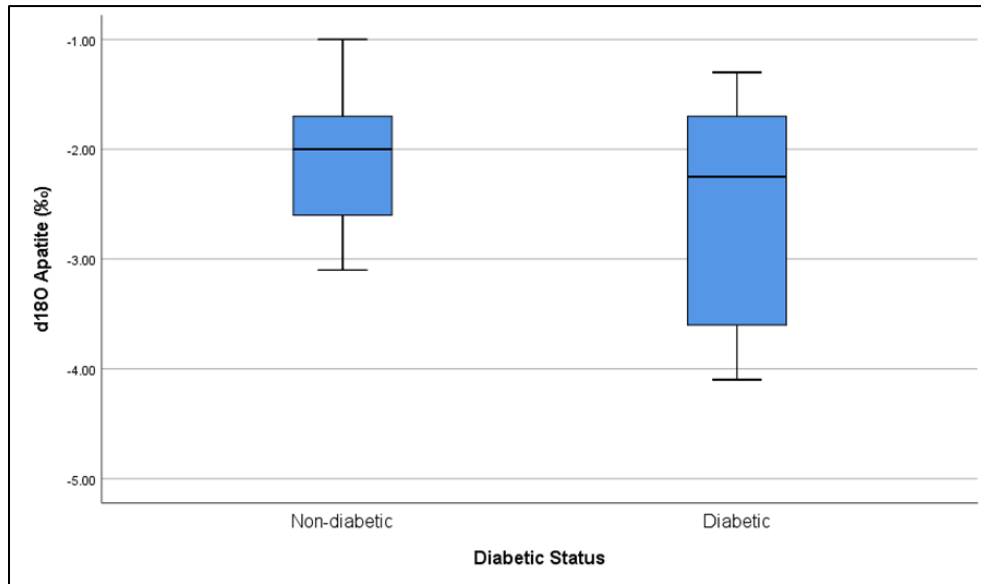


**Figure 9.** Box plots of non-diabetics' and diabetics' apatite  $\delta^{18}\text{O}$ .

In case the difference between Austin, Texas and San Antonio, Texas average tap water  $\delta^{18}\text{O}$  has a significant effect on donors' apatite  $\delta^{18}\text{O}$ , residents were statistically analyzed separately. All sub samples were tested for the assumption of normality prior to statistical analyses. A K-S test revealed that apatite  $\delta^{18}\text{O}$  of non-diabetics within Austin, Texas is normal ( $n = 7$ , mean = -2.200, SD = 0.741,  $p = 0.200$ ). Since the sub sample of diabetics within Austin, Texas is less than five, a Shapiro-Wilk test was conducted to test for normality, which revealed a normal distribution ( $n = 3$ , mean = -2.200, SD = 1.228,  $p = 0.312$ ). Since all sub samples within Austin, Texas (Table 6) are distributed normally,

visual inspection of boxplots (Figure 10) and an independent sample t-test were used to test if the average apatite  $\delta^{18}\text{O}$  of diabetics and non-diabetics differed among Austin, Texas residents. The independent sample t-test revealed apatite  $\delta^{18}\text{O}$  average values of non-diabetics was not different to diabetics' apatite  $\delta^{18}\text{O}$  ( $p = 0.249$ ,  $t < 0.001$ ,  $df = 8$ ). Levene's test indicated equal variances ( $F = 1.549$ ,  $p = 0.249$ ).

**Table 6.** Descriptive statistics of apatite  $\delta^{18}\text{O}$  to donors from Austin, Texas.

	Diabetic Status	N	Mean	Std. Deviation	Std. Error Mean
$\delta^{18}\text{O}$ Apatite	Non-diabetic	7	-2.2000	0.74162	0.28031
	Diabetic	3	-2.2000	1.22882	0.70946

a. Donor Residence = Austin

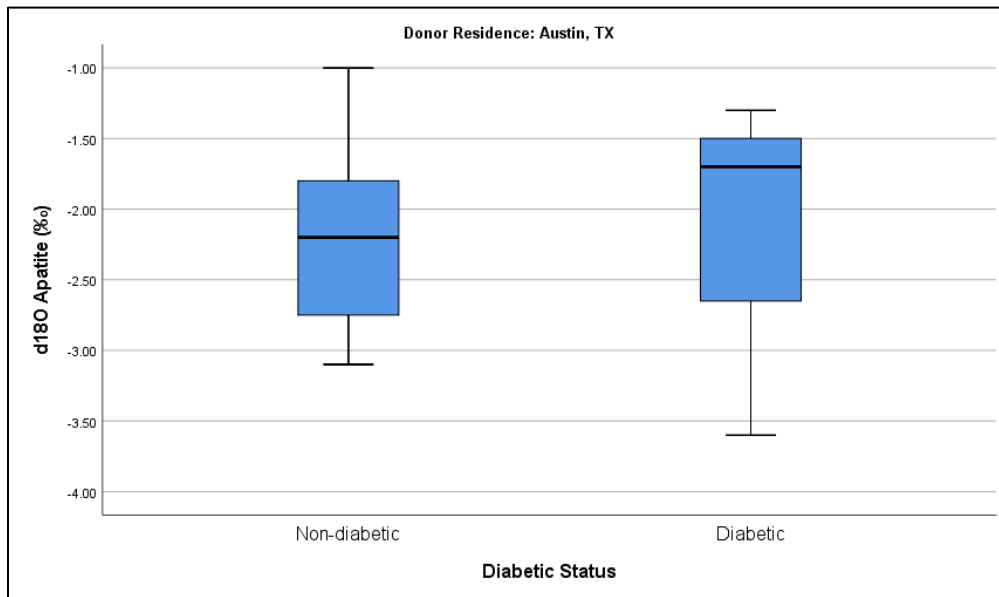


**Figure 10.** Box plots comparing apatite  $\delta^{18}\text{O}$  values of non-diabetics to diabetics within Austin, Texas (TX).

Should differences in San Antonio, Texas tap water  $\delta^{18}\text{O}$  have a significant effect on donors' apatite  $\delta^{18}\text{O}$ , San Antonio residents were statistically analyzed separately. Since the sub samples of non-diabetics ( $n = 4$ ) and diabetics ( $n = 3$ ) within San Antonio, Texas are less than five, assumptions for normality were tested by Shapiro-Wilk statistical analysis. A Shapiro-Wilk test for normality revealed that the sub-sample of apatite  $\delta^{18}\text{O}$  to non-diabetics from San Antonio, Texas is normally distributed ( $n = 4$ , mean = -2.00, SD = 0.432,  $p = 0.577$ ). A Shapiro-Wilk test for normality revealed that the sub sample of apatite  $\delta^{18}\text{O}$  to diabetics from San Antonio, Texas is also distributed normally ( $n = 3$ , mean = -2.866, SD = 1.069,  $p = 0.089$ ). Since subsamples within San Antonio, Texas (Table 7) are normal, visual inspection of boxplots (Figure 11) and independent sample t-tests were used to test if the average apatite  $\delta^{18}\text{O}$  of diabetics and non-diabetics differed among San Antonio, Texas residents. The independent sample t-test revealed diabetics' apatite  $\delta^{18}\text{O}$  average is lower to non-diabetics  $\delta^{18}\text{O}$  apatite average within San Antonio, Texas, and approaches significance ( $p = 0.074$ ,  $t = 1.504$ ,  $df = 5$ ). Levene's test indicated equal variances ( $F = 5.098$ ,  $p = 0.074$ ).

**Table 7.** Descriptive statistics of apatite  $\delta^{18}\text{O}$  values of donors from San Antonio, Texas.

Group Statistics <sup>a</sup>					
	Diabetic Status	N	Mean	Std. Deviation	Std. Error Mean
$\delta^{18}\text{O}$ Apatite	Non-diabetic	4	-2.0000	0.43205	0.21602
	Diabetic	3	-2.8667	1.06927	0.61734

a. Donor Residence = San Antonio, Texas

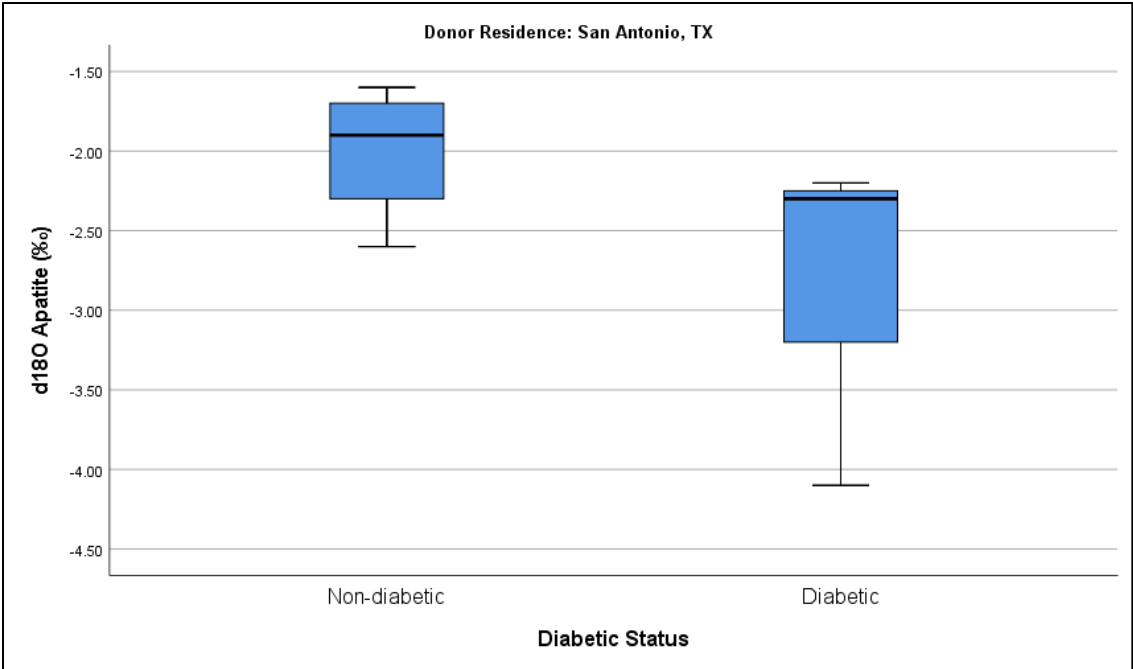


**Figure 11.** Box plots comparing apatite  $\delta^{18}\text{O}$  values of non-diabetics to diabetics within San Antonio, Texas (TX).

## V. DISCUSSION

In overview, the purpose of this thesis was to conduct an exploratory study on the effect of underlying diabetes mellitus (DM) on stable oxygen isotopic ratios ( $\delta^{18}\text{O}$ ).

Isotopic data from skeletonized donors with known DM history to donors with no biographical indication of DM were observed to assess whether differences in population averages exist. Independent sample t-test analyses were conducted on subgroups to quantify whether data suggest isotopic ratios reflect two different populations.

### **Water Surveys**

Box plots of the raw tap  $\delta^{18}\text{O}$  data visually express a narrower range of values from Austin, Texas when compared to San Antonio, Texas. This difference in distribution size may be due to differences in the quantity of tap water sources within the two cities. Austin, Texas tap water is primarily sourced by the Colorado, River; San Antonio, Texas tap water is sourced by the Edwards, Carrizo, Trinity, and Wilcox aquifers, and in some areas, Canyon Lake (SAWS, 2021). Additional factors contributing to variability in tap water  $\delta^{18}\text{O}$  consist of differences in source to consumer treatment and the assumption that the contribution of water from each water source may change over time (Chesson et al., 2010).

### **Isoscapes**

Statistical analysis used to map tap water  $\delta^{18}\text{O}$  as an isoscape accounts for the weighted differences between known data points. Overall average tap  $\delta^{18}\text{O}$  extracted from the isoscape accounts for the average of raw data and estimated values between the distances of raw data. However, outliers in raw data may skew the estimated between-distance data when creating an isoscape. For this reason, it is suggested for the average of

the area of interest to be extracted opposed to the tap  $\delta^{18}\text{O}$  per cell within a raster. Additionally, it is less common for researchers to sample identical latitude and longitudinal coordinates over time unless a specific research question calls for the methodology such as controlling variability to observe temporal or seasonal changes. Extracting the tap water  $\delta^{18}\text{O}$  value per cell would often result on data statistically computed by a singular tap water sample, which is less likely to reflect the true mean of overall tap water  $\delta^{18}\text{O}$  for the area.

### **Contribution to Anthropology**

Isoscapes are a useful tool in forensic anthropology to estimate the region of origin of unknown individuals by their apatite  $\delta^{18}\text{O}$ . The chemical signatures preserved in bone can be used to trace probable origins through similarities to the chemical signatures preserved in the environment and accounting for diet, confidence interval, and isotopic fractionation. The tap water data collected as part of this thesis have contributed to more precise isoscapes of metro-areas Austin, Texas and San Antonio, Texas, which may aid in geo-location methodologies of modern populations. This work contributes to work towards refinement of isoscapes across the United States (Bowen et al., 2007; Warner et al., 2018). An essential asset of this method is applicability of various human tissues (e.g., hair, nails, dentition, bone) which reflect different life history intervals. Additionally, this method provides a useful tool for comingled, fragmented, or isolated elements. Estimating region of origin by stable isotope analysis contributes to identification efforts when compiled with the biological profile and may enable distinguishment between individuals when remains are comingled. (Warner et al., 2018).

As stable isotope analysis becomes more widely used amongst archaeologists and forensic scientists, it is important to consider how physiological stress and potentially metabolic disease may alter the chemical signature preserved in tissues (Chesson et al., 2018). As previously discussed, apatite  $\delta^{18}\text{O}$  is most correlated with drinking water while also reflecting oxygen from foods and respiration. Tap water collected as part of this thesis reflect donors' proximate tap water  $\delta^{18}\text{O}$  and their city's average  $\delta^{18}\text{O}$ , which provides a comparable basis for disruptions in source of inference, and thus geolocation, due to underlying DM. Additionally, it is commonly generalized for bone to reflect the past 10-20 years of life, however, bone turn-over-rate is not a constant (Bartelink & Chesson, 2019). The rib element may reflect the average life history of about 5-10 years before death depending on the individual's rate of remodeling (e.g., age, health). Donors used as part of this thesis consist of a known residential history ranging from 6-64 years before death (Table 1), which provides opportunity to observe effect of residential duration on isotopic signature, if any.

### **Apatite $\delta^{18}\text{O}$**

Diabetic donors' apatite  $\delta^{18}\text{O}$  was lower than non-diabetics among San Antonio residents, however, this difference is not statistically significant, whereas diabetic donors' apatite  $\delta^{18}\text{O}$  was like non-diabetics among Austin, Texas residents. It is important to note the three known diabetic donors who reside in Austin, Texas have either not been diagnosed with diabetes for a period longer than four years before death or have not resided in Austin, Texas for longer than six years. Donor 2013.014 has a known diabetic onset period of four years before death and donor 2016.038 has a known diabetic onset of two years before death. Nonetheless, all data known to period of onset relates the

*minimum* number of years the individual expressed diabetes mellitus as symptoms of diabetes may have been experienced for unknown duration prior to diagnosis. The third and final diabetic donor from Austin, Texas, 2014.062, has a known 20-year period of onset, however, only resided in Austin, Texas for six years before death. It is possible donor 2014.062's apatite  $\delta^{18}\text{O}$  is still more like their previous tap  $\delta^{18}\text{O}$  residence than to Austin, Texas. Short residency and short period of onset are two factors which may influence the effect of the underlying condition on apatite  $\delta^{18}\text{O}$ .

The lower apatite  $\delta^{18}\text{O}$  among diabetics who reside in San Antonio, Texas compared to non-diabetics may be due to diabetics with longer periods of onset. Two of the three known diabetics from San Antonio, Texas have known medical onset data related to their DM. Donor 2015.004 has a known onset period of 10 years before death, 10-year residency, and apatite  $\delta^{18}\text{O}$  of -2.20. Donor 2014.007 has a known onset period of 11 years before death, 21-year residency, and an apatite  $\delta^{18}\text{O}$  of -4.10. It is possible for donor 2014.007's apatite  $\delta^{18}\text{O}$  to be more like the average tap  $\delta^{18}\text{O}$  of San Antonio, -4.06, due to a longer period of residency in San Antonio, thus a longer period for bone tissue turnover to reflect the individual's diet and drinking water 10-20 years before death. The final diabetic donor from San Antonio, Texas (2010.013) has a residency of 17 years before death, however, has an unknown period diabetic onset. If correlations can be made between differences in apatite  $\delta^{18}\text{O}$  of diabetics with known onset periods, these trends can be used to predict an estimated number of years a diabetic suffered from DM whose period of onset was otherwise unknown. Further research and robust sampling are recommended to confirm certainty of any of the observations discussed.

The use of donors with the Texas State Donated Skeletal Collection enables research of direct pathology-related variations on isotopic ratios. The use of a skeletal collection with known demographic, residential, and medical histories allow researchers to further discriminate if overall trends remain consistent when factors such as sex and age are incorporated in statistical analyses. Additional sampling is recommended to encompass a sample size large enough to compare demographics within the sample. If demographic parameters, residency, and diet can be accounted for as constants, then it is more likely for the variation in apatite  $\delta^{18}\text{O}$  be due to underlying disease.

Furthermore, apatite  $\delta^{18}\text{O}$  does not statistically differ within samples. Since this chemical signature is most correlated to drinking water, it may be that the 2-3‰ difference in tap  $\delta^{18}\text{O}$  between San Antonio, Texas and Austin, Texas will not statistically affect expected apatite  $\delta^{18}\text{O}$ . Further research is recommended to estimate the expected apatite  $\delta^{18}\text{O}$  of all donors with their corresponding tap  $\delta^{18}\text{O}$ . The predicted values can be statistically compared to each donors' observed apatite  $\delta^{18}\text{O}$  and may then reveal any statistical difference due to a 2-3‰ difference in drinking water  $\delta^{18}\text{O}$ .

Finally, diabetes mellitus (DM) is a condition which affects non-Asian minority groups at a higher prevalence to white or Asian groups. DM also affects individuals of lower socio-economic status within ethnic groups at a higher prevalence. All donors used in this thesis are self-identified as American White, however, their residential data may reflect differences in socio-economic status. Education and income are two factors contributing to socio-economic status. According to the US Census Bureau, as of 2019, 51.7% of Austin, Texas residents held a bachelor's degree or higher. The median household income was \$71,576 from 2015-2019. As of 2019, 26% of San Antonio, Texas

residents held a bachelor's degree or higher. The median household income between 2015-2019 was \$52,455. In 2019, the poverty rate in Austin, Texas was 13.2% compared to a poverty rate of 17.8% in San Antonio, Texas. A lower socio-economic background of donors from San Antonio, Texas compared to those from Austin, Texas may suggest differences in healthcare access. These data are essential when attributing differences in apatite  $\delta^{18}\text{O}$  of diabetics to non-diabetics. Further research is recommended to assess whether there are significant differences in apatite  $\delta^{18}\text{O}$  and whether these differences are due to the period an individual expressed DM or if the differences are attributed to the irregular treatment of DM as reflected by healthcare access.

## VI. FUTURE RESEARCH

As previously mentioned, this thesis discusses results to rib samples of 17 donors. Future directions include the addition of data for seven remaining samples (Appendix E) as approved by the Forensic Anthropology Board and estimating diet and nutrition to further assess the condition of underlying disease. Assessments of diet and nutrition will be observed by a multi-isotope analysis of bone collagen. Statistical analyses will also be conducted with the addition of data to the seven donors to help determine if differences in apatite  $\delta^{18}\text{O}$  continue to approach statistical significance ( $p < .05$ ).

Compilation of data will increase sample size of diabetics and non-diabetics which is anticipated to clarify the existence of trend patterns. Specifically, two of the additional seven donors are diabetics from Austin, Texas. Ideally, this additional data will strengthen patterns between diabetic apatite  $\delta^{18}\text{O}$  ratios to non-diabetic apatite  $\delta^{18}\text{O}$  and clarify whether the visually observed patterns within San Antonio residents can also be found among Austin, Texas residents.

Moreover, current tap water data are curated at [waterisotopes.org](https://waterisotopes.org) database along with current raster grids. The updated raster grids consist of tap water stable oxygen isotope ratio ( $\delta^{18}\text{O}$ ) data formatted into rows and columns across the United States. Cells within the rows and columns represent a data value following Bowen et al. (2007) along with current accessible data found at <https://waterisotopesDB.org> on 6/8/2021. The author will generate new raster grids including all current data available at [waterisotopes.org](https://waterisotopes.org) following the script found at [waterisotopes.org](https://waterisotopes.org). The creation of isoscapes with the implementation of the R script will maintain the standardization of tap water maps across the United States.

Standardization of water data will also allow the author to calculate expected values of apatite stable oxygen isotope ratio ( $\delta^{18}\text{O}$ ) of donors analyzed for isotopic analysis using their associated tap water  $\delta^{18}\text{O}$  data in mass balance equations (Podlesak et al., 2012). A comparison of observed to expected apatite  $\delta^{18}\text{O}$  will provide a better understanding of whether differences are due to variety in water source or if differences are attributed to metabolic disease. Expansion of statistical analyses will also be conducted to assess statistical differences in observed to expected apatite  $\delta^{18}\text{O}$ .

## VII. CONCLUSION

Tap water samples collected for this thesis resulted in a robust water survey of metro areas San Antonio, Texas and Austin, Texas and were compiled with tap water data curated at [waterisotopes.org](http://waterisotopes.org). These compiled surveys are more likely to reflect the true mean of the area as compounded surveys are less prone to seasonal and temporal bias.

The apatite  $\delta^{18}\text{O}$  ratios of diabetics are like apatite  $\delta^{18}\text{O}$  of non-diabetics within Austin, Texas. Diabetics' apatite  $\delta^{18}\text{O}$  are lower to non-diabetics' apatite  $\delta^{18}\text{O}$  within San Antonio, Texas. Overall, diabetics altogether express a lower apatite  $\delta^{18}\text{O}$  mean to non-diabetics, however, insignificantly so ( $p = 0.092$ ); thus, we fail to reject the null that diabetics would express a different apatite  $\delta^{18}\text{O}$  to non-diabetics. Further research is recommended to decipher whether the duration of underlying pathology, the regularity of insulin among individuals of different socioeconomic status, and/or whether potential access to healthcare is influencing any observed trending patterns.

The results of this research indicate observed variation in apatite  $\delta^{18}\text{O}$  among donors, however, there is no strong evidence of correlation with known diabetes mellitus. Data collected as part of this thesis will be explored further by implementing a multi-isotope approach, which will provide additional data for the author and colleagues to interpret in correlation with DM pathology. Future directions of this research will highlight a multi-disciplinary approach in ecology, biological anthropology, and chemistry to provide a more holistic osteobiography of the donors contributing to this explorative study.

## APPENDIX SECTION

**APPENDIX A.** Summary of curated data to water samples collected from Austin, Texas and San Antonio, Texas found at [waterisotopes.org](http://waterisotopes.org).

Site Name	Latitude	Longitude	d18O	Source
Steph_s house	30.195751	-97.780336	-1.182540321	Attn: Melanie Beasley
Hampton	30.2640926	-97.74197715	-2.835356914	Unpublished, Attn: Gabe Bowen
Austins Inn	30.282896	-97.747141	-1.895423095	Attn: Gabe Bowen
East Austin	30.31460027	-97.69728702	-2.90145284	Attn: Gabe Bowen
Austin, TX	30.336	-97.663	-2.02	Coplen et al., 2013
Austin, TX	30.336	-97.663	-2.27	Coplen et al., 2013
EDC airport	30.39996246	-97.57335193	-2.155032309	Attn: Gabe Bowen
AT	30.2669	-97.7428	-1.915049377	Kennedy et al., 2011
AT	30.2669	-97.7428	-1.988528226	Kennedy et al., 2011
AT	30.2669	-97.7428	-1.951211799	Kennedy et al., 2011
AT	30.2669	-97.7428	-2.580296232	Kennedy et al., 2011
AT	30.2669	-97.7428	-8.155328276	Kennedy et al., 2011
AT	30.2669	-97.7428	-2.569526919	Kennedy et al., 2011
AT	30.2669	-97.7428	-2.475930434	Kennedy et al., 2011
AT	30.2669	-97.7428	-8.990402899	Kennedy et al., 2011
AT	30.2669	-97.7428	-2.405152268	Kennedy et al., 2011
AT	30.2669	-97.7428	-2.397285005	Kennedy et al., 2011
AT	30.2669	-97.7428	-2.51161758	Kennedy et al., 2011
AT	30.2669	-97.7428	-2.5552897	Kennedy et al., 2011
AT	30.2669	-97.7428	-2.649477233	Kennedy et al., 2011
AT	30.2669	-97.7428	-2.468077293	Kennedy et al., 2011
AT	30.2669	-97.7428	-2.477969004	Kennedy et al., 2011
AT	30.2669	-97.7428	-1.850397615	Kennedy et al., 2011

<b>Site Name</b>	<b>Latitude</b>	<b>Longitude</b>	<b>d18O</b>	<b>Source</b>
AT	30.2669	-97.7428	-1.333259512	Kennedy et al., 2011
AT	30.2669	-97.7428	-0.909983626	Kennedy et al., 2011
AT	30.2669	-97.7428	-0.834453008	Kennedy et al., 2011
AT	30.2669	-97.7428	-1.37033233	Kennedy et al., 2011
AT	30.2669	-97.7428	-1.534014153	Kennedy et al., 2011
AT	30.2669	-97.7428	-1.185483648	Kennedy et al., 2011
AT	30.2669	-97.7428	-1.030829075	Kennedy et al., 2011
AT	30.2669	-97.7428	-0.603307608	Kennedy et al., 2011
AT	30.2669	-97.7428	-0.949978155	Kennedy et al., 2011
AT	30.2669	-97.7428	-0.094024034	Kennedy et al., 2011
AT	30.2669	-97.7428	-0.272173103	Kennedy et al., 2011
SAT airport	29.52841	-98.4725	-4.33246	Unpublished, attn: Gabe Bowen
San Antonio, TX	29.563	-98.594	-3.92	Coplen et al., 2013
San Antonio, TX	29.563	-98.594	-3.81	Coplen et al., 2013
Hotel Contessa	29.4232	-98.4896	-4.2381	Unpublished, attn: Gabe Bowen
USATXSan Antonio	29.4239	-98.4933	-3.00924	Unpublished, attn: Isoforensics Inc.
USATXSan Antonio	29.4239	-98.4933	-2.83769	Unpublished, attn: Isoforensics Inc.
USATXSan Antonio	29.4239	-98.4933	-4.21166	Unpublished, attn: Isoforensics Inc.
USATXSan Antonio	29.4239	-98.4933	-4.38527	Unpublished, attn: Isoforensics Inc.

**APPENDIX B.** Accessible tap water stable oxygen isotope ratio ( $\delta^{18}\text{O}$ ) data to Texas in Waterisotopes Database (2021)  
<http://waterisotopesDB.org>. Accessed 6/19/2021. Query: Country=US, State/Province=TX, Type=Tap.

Site Name	Latitude	Longitude	Sample Comments	$\delta^{18}\text{O}$	Project ID
K Bar Ranch House	29.30552	-103.178		-7.48743	3
Panther Junction	29.32773	-103.206		-7.46939	3
Wildcatter Aviation	31.92276	-102.393		-0.27154	3
Comfort Suites Odessa	31.89994	-102.337		-0.28599	3
Shell	32.76097	-94.3553		-1.74997	183
Exxon	31.94601	-94.2394		-5.01762	183
Super 8 Motel	30.38356	-94.3167		-4.04266	183
Valero	29.69783	-95.2025		-2.45191	183
Kari_s parent_s house	29.75394	-95.7315		-4.79172	183
Steph_s house	30.19575	-97.7803		-1.18254	183
Shell	31.05409	-97.4547		-1.26133	183
Waco Mammoth NM Vistor Center	31.60677	-97.176		-0.96465	183
Shell	32.24359	-96.4971		0.16219	183
Valero	32.34697	-95.3165		-5.72276	183
IAH airport	29.98574	-95.3361		-4.51927	99
IAH airport	29.98574	-95.3361		-4.55062	99
IAH airport	29.98574	-95.3361		-4.41782	99
Hotel Contessa	29.4232	-98.4896		-4.2381	99
SAT airport	29.52841	-98.4725		-4.33246	99
IAH airport	29.98574	-95.3361		-4.55633	99

Site Name	Latitude	Longitude	Sample Comments	$\delta^{18}\text{O}$	Project ID
IAH airport	29.98574	-95.3361		-4.45763	99
Hampton	30.26409	-97.742		-2.83536	99
T78 airport	30.08012	-94.6977		-4.6858	225
6R3 airport	30.35968	-95.0079		-4.44	225
UTS airport	30.7429	-95.5861		-3.77712	225
60R airport	30.37377	-96.1146		-4.54902	225
GYB airport	30.17055	-96.9791		-5.16069	225
EDC airport	30.39996	-97.5734		-2.15503	225
East Austin	30.3146	-97.6973		-2.90145	225
Airport Diner	30.24443	-98.908		-3.70702	225
JCT airport	30.51025	-99.7656		-4.75283	225
OZA airport	30.7313	-101.203		-5.60591	225
INK airport	31.7828	-103.196		-5.91293	225
PEQ airport	31.39	-103.511		-6.98362	225
VHN airport	31.06086	-104.786		-7.81255	225
Wyndham	31.79669	-106.398		-10.4143	225
IAH airport	29.98574	-95.3361		-4.56812	99
7-11 store	32.75906	-96.8205		-1.686	225
Victory Forest	32.4158	-97.1948		-1.49834	225
Ray St	32.37788	-97.3322		-5.53572	225
Short St	32.34147	-97.4275		-1.17612	225
Moccasin Dr	33.06917	-96.7153		-1.89099	225
N Creek Circle	32.46954	-96.8118		-1.28812	225
Gas station	32.66159	-96.8917		-1.64113	225
Jack in the Box	32.79195	-96.7506		-1.62576	225
Austins Inn	30.2829	-97.7471		-1.89542	225
Bay Meadows Dr	32.96677	-97.1298		-0.64694	225

Site Name	Latitude	Longitude	Sample Comments	$\delta^{18}\text{O}$	Project ID
Cheshire St	32.62557	-97.3436		-1.65602	225
Summit Ave	32.7327	-97.1213		-1.49409	225
Willow Springs	32.63944	-97.1718		-1.47495	225
McDonalds	32.98794	-96.8417		-1.4707	225
QT gas station	32.46013	-96.8422		-1.30944	225
Pinnacle Bank	32.7587	-97.1139		-1.63699	225
Heahtherbrook Dr	32.64453	-97.1632		-1.51213	225
Stutz Dr	32.82205	-96.8386		-1.53091	225
Pac N Sac Gas Station	29.87639	-97.9286		-3.43287	225
The Woods Apt Complex	29.87248	-97.9289		-3.3596	225
The Comfort Inn & Suites	29.8691	-97.9375		-3.41293	225
San Marcos DMV	29.89025	-97.9137		-3.38507	225
Mochas and Javas	29.89194	-97.9397	Water fountains	-3.46056	225
Evans Liberal Arts Building on Texas State University Campus	29.89222	-97.9464	Womens bathroom	-4.22379	225
Academy	29.84818	-97.9682	Restroom sink	-3.504	225
Englebrook Apartments	29.88208	-97.94	kitchen sink	-3.38159	225
Codys Bistro	29.8282	-97.9874	Restroom sink	-3.44085	225
Texas State University Greenhouse	29.88609	-97.9466	Restroom sink	-4.23794	225

Site Name	Latitude	Longitude	Sample Comments	$\delta^{18}\text{O}$	Project ID
Texas State University Comal Building	29.88934	-97.9409	Restroom sink	-4.253	225
Mochas and Javas in HEB	29.8873	-97.9263	restaunt sink	-3.40075	225
Hobby Lobby	29.88306	-97.9172	Womens bathroom	-3.4359	225
Iconic Village Apartments 100 Building	29.89669	-97.9419	bathroom sink	-3.81215	225
St. Marks Episcopal Church	29.9046	-97.9958	Restroom sink	-4.40978	225
Alpha Sigma Phi Fraternity House	29.9067	-98.0069	Sink	-4.24506	225
Lower Purgatory Creek trailhead	29.86572	-97.9642	tallest water fountain	-3.4203	225
The Pita Shop	29.89863	-97.971	Womens bathroom	-3.87391	225
Walgreens	29.89685	-97.9647		-3.67124	225
The Grove Apartments	29.90194	-97.9025	kitchen sink	-3.42584	225
7-Eleven Gas Station	29.85583	-97.9528	Womens bathroom	-3.42081	225
Texaco	29.89706	-97.9218	unisex bathroom	-3.45619	225
Sewell Park Outdoor Center	29.88732	-97.9337	Womens bathroom	-4.26454	225
Sunco Gas Station	29.8997	-97.9078	Womens bathroom	-3.41997	225
The Meadows Center for Water and the Environment	29.89389	-97.9294		-3.40085	225

Site Name	Latitude	Longitude	Sample Comments	$\delta^{18}\text{O}$	Project ID
San Marcos Activity Center	29.88472	-97.9322	Water fountains	-3.43498	225
Burger King	29.86689	-97.9391	Mens bathroom sink	-3.37967	225
Walmart	29.88325	-97.9137	Mens Restroom sink	-3.40262	225
Rio Grande Village Camp	29.18044	-102.956		-7.40727	3
Panther Junction	29.32773	-103.206		-7.18794	3
La Quinta	30.8986	-102.909		-7.92484	3
USATXAbilene	32.4	-99.7	Old ID: 32408	3.166667	275
USATXCollege Station	30.6	-96.3	Old ID: 32410	-1.44571	275
USATXWichita Falls	34	-98.5	Old ID: 32411	4.2	275
USATXDallas	32.8	-96.8	Old ID: 32412	-0.28586	275
USATXCanyon	35	-101.9	Old ID: 32413	-3.46589	275
USATXLubbock	33.7	-101.8	Old ID: 32417	0.412896	275
USATXEl Paso	31.8	-106.5	Old ID: 51714	-9.92059	275
USATXAlpine	30.4	-103.7	Old ID: 51715	-6.40156	275
San Angelo	31.5	-100.4	Old ID: 51718	1.721079	275
USATXWaco	31.5	-97.1	Old ID: 51719	-2.84294	275
USATXDumas	35.9	-102	Old ID: 51717	-7.22	275
USATXCorpus Christi	27.73898	-97.4361	Old ID: 51721	-4.03188	275
USATXHouston	29.76	-95.36	Old ID: 42453		
USATXPecos	31.4263	-103.494	Old ID: Water #22	-6.95651	275
USATXPecos	31.4198	-103.492	Old ID: Water #23	-6.85901	275
USATXPecos	31.4156	-103.49	Old ID: Water #24	-6.9133	275
USATXOdessa	31.8423	-102.366	Old ID: Water #25	0.206524	275

Site Name	Latitude	Longitude	Sample Comments	$\delta^{18}\text{O}$	Project ID
USATXOdessa	31.8552	-103.375	Old ID: Water #26	0.132619	275
USATXOdessa	31.8552	-103.375	Old ID: Water #27	0.691902	275
USATXBig Spring	32.25	-101.479	Old ID: Water #28	0.574571	275
USATXBig Spring	32.25	-101.479	Old ID: Water #29	0.318537	275
USATXBig Spring	32.25	-101.479	Old ID: Water #30	0.936175	275
USATXSan Angelo	31.4198	-100.441	Old ID: Water #31	1.325974	275
USATXSan Angelo	31.4255	-100.497	Old ID: Water #32	1.607285	275
USATXSan Angelo	31.4253	-100.495	Old ID: Water #33	1.610471	275
USATXKerrville	30.0667	-99.1647	Old ID: Water #34	-4.46607	275
USATXKerrville	30.0667	-99.1647	Old ID: Water #35	-4.93312	275
USATXKerrville	30.0667	-99.1632	Old ID: Water #36	-4.21848	275
USATXSan Antonio	29.4239	-98.4933	Old ID: Water #37	-4.38527	275
USATXLuling	29.6818	-97.6494	Old ID: Water #38	-3.84515	275
USATXLuling	29.6494	-97.6494	Old ID: Water #39	-3.39613	275
USATXLuling	29.6494	-97.6494	Old ID: Water #40	-4.02188	275
USATXColumbus	29.706	-96.5468	Old ID: Water #41	-4.97805	275
USATXColumbus	29.706	-96.5468	Old ID: Water #42	-3.44274	275
USATXColumbus	29.706	-96.5468	Old ID: Water #43	-4.7708	275
USATXAmarillo	35.2219	-101.831	Old ID: Water #73	-4.20661	275
USATXAmarillo	35.2219	-101.831	Old ID: Water #74	-4.61588	275
USATXAmarillo	35.2219	-101.831	Old ID: Water #75	-4.3373	275

Site Name	Latitude	Longitude	Sample Comments	$\delta^{18}\text{O}$	Project ID
USANMDalhart	36.0606	-102.348	Old ID: Water #76	-6.69365	275
USANMDalhart	36.0606	-102.348	Old ID: Water #77	-7.34258	275
USANMDalhart	36.0606	-102.348	Old ID: Water #78	-6.92444	275
USATXArnot	35.18932	-102.011	Old ID: ANTTX0408	-6.94661	275
USATXAlanreed	35.2144	-100.74	Old ID: ALRTX0409	-5.7315	275
USATXAmarillo	35.2219	-101.831	Old ID: DL120520021001	-2.38691	275
USATXAmarillo	35.2219	-101.831	Old ID: DL120520021002	-2.22754	275
USATXAmarillo	35.2219	-101.831	Old ID: DL120520021003	-2.26835	275
NT hom	32.7833	-96.8	Old ID: NT home 04/05	-1.84478	275
USATXHouston	29.7631	-95.3631	Old ID: PC home 08/05	-1.50088	275
	27.5013	-99.4369	Old ID: JB 01	-2.84299	275
	32.89667	-97.0381	Old ID: JB 03	0.172622	275
	30.0858	-94.1017	Old ID: Trip03_W3003	-3.44499	275
USATXHouston	29.7631	-95.3631	Old ID: Trip03_W3016	-2.70431	275
USATXHouston	29.7631	-95.3631	Old ID: Trip03_W3017	-2.6634	275
USATXHouston	29.7631	-95.3631	Old ID: Trip03_W3018	-2.61666	275
USATXSan Antonio	29.4239	-98.4933	Old ID: Trip03_W3020	-3.00924	275

Site Name	Latitude	Longitude	Sample Comments	$\delta^{18}\text{O}$	Project ID
USATXSan Antonio	29.4239	-98.4933	Old ID: Trip03_W3027	-2.83769	275
USATXSan Antonio	29.4239	-98.4933	Old ID: Trip03_W3028	-4.21166	275
USATXHouston	29.7631	-95.3631	Old ID: Trip03_W3030	-2.77277	275
AT	30.2669	-97.7428	Old ID: Trip03_W3031	-1.91505	275
AT	30.2669	-97.7428	Old ID: Trip03_W3038	-1.98853	275
AT	30.2669	-97.7428	Old ID: Trip03_W3039	-1.95121	275
	31.4675	-97.1144	Old ID: Trip03_W3041	-3.91101	275
NT hom	32.7833	-96.8	Old ID: Trip03_W3042	-1.4538	275
NT hom	32.7833	-96.8	Old ID: Trip03_W3043	-1.53231	275
NT hom	32.7833	-96.8	Old ID: Trip03_W3044	-1.56875	275
NT hom	32.7833	-96.8	Old ID: Trip03_W3057	-0.71989	275
	31.7586	-106.486	Old ID: Trip02_W2001	-9.88976	275
	31.7586	-106.486	Old ID: Trip02_W2002	-11.6872	275
	31.7586	-106.486	Old ID: Trip02_W2016	-11.5972	275

Site Name	Latitude	Longitude	Sample Comments	$\delta^{18}\text{O}$	Project ID
	31.0399	-104.831	Old ID: Guadalupe Mountains tap	-9.12453	275
	30.894	-102.879	Old ID: Fort Stockton tap	-7.84236	275
	30.711	-101.212	Old ID: Ozona tap	-4.57909	275
	30.4894	-99.772	Old ID: Junction tap	-4.5276	275
	30.093	-93.7366	Old ID: Orange tap	-4.45337	275
	32.897	-97.038	Old ID: Dallas-Fort Worth tap	-2.37845	275
	30.2672	-97.7431	Old ID: Austin, TX tap	-1.63772	275
	31.5493	-97.1467	Old ID: 2012 SIE 03	-3.38429	275
	30.628	-96.3344	Old ID: 2012 SIE 32	-5.06245	275
NT hom	32.7833	-96.8	published by Kennedy et al., 2011, FSI	-1.20783	46
PC hom	29.7631	-95.3631	published by Kennedy et al., 2011, FSI	-2.44798	46
PC chu	29.7631	-95.3631	published by Kennedy et al., 2011, FSI	-2.23221	46
AT	30.2669	-97.7428	published by Kennedy et al., 2011, FSI	-2.5803	46

Site Name	Latitude	Longitude	Sample Comments	$\delta^{18}\text{O}$	Project ID
AT	30.2669	-97.7428	published by Kennedy et al., 2011, FSI	-8.15533	46
AT	30.2669	-97.7428	published by Kennedy et al., 2011, FSI	-2.56953	46
NT hom	32.7833	-96.8	published by Kennedy et al., 2011, FSI	-1.74607	46
PC hom	29.7631	-95.3631	published by Kennedy et al., 2011, FSI	-2.42309	46
PC chu	29.7631	-95.3631	published by Kennedy et al., 2011, FSI	-2.65462	46
AT	30.2669	-97.7428	published by Kennedy et al., 2011, FSI	-2.47593	46
PC hom	29.7631	-95.3631	published by Kennedy et al., 2011, FSI	-2.88437	46
PC chu	29.7631	-95.3631	published by Kennedy et al., 2011, FSI	-2.69862	46
NT hom	32.7833	-96.8	published by Kennedy et al., 2011, FSI	-1.02196	46

Site Name	Latitude	Longitude	Sample Comments	$\delta^{18}\text{O}$	Project ID
NT hom	32.7833	-96.8	published by Kennedy et al., 2011, FSI	-1.84478	46
AT	30.2669	-97.7428	published by Kennedy et al., 2011, FSI	-8.9904	46
AT	30.2669	-97.7428	published by Kennedy et al., 2011, FSI	-2.40515	46
PC hom	29.7631	-95.3631	published by Kennedy et al., 2011, FSI	-2.84912	46
PC chu	29.7631	-95.3631	published by Kennedy et al., 2011, FSI	-2.8967	46
AT	30.2669	-97.7428	published by Kennedy et al., 2011, FSI	-2.39729	46
NT hom	32.7833	-96.8	published by Kennedy et al., 2011, FSI	-0.56191	46
PC hom	29.7631	-95.3631	published by Kennedy et al., 2011, FSI	-2.3893	46
PC chu	29.7631	-95.3631	published by Kennedy et al., 2011, FSI	-2.22426	46

Site Name	Latitude	Longitude	Sample Comments	$\delta^{18}\text{O}$	Project ID
AT	30.2669	-97.7428	published by Kennedy et al., 2011, FSI	-2.51162	46
NT hom	32.7833	-96.8	published by Kennedy et al., 2011, FSI	-0.28941	46
PC hom	29.7631	-95.3631	published by Kennedy et al., 2011, FSI	-2.45322	46
PC chu	29.7631	-95.3631	published by Kennedy et al., 2011, FSI	-2.99151	46
AT	30.2669	-97.7428	published by Kennedy et al., 2011, FSI	-2.55529	46
PC hom	29.7631	-95.3631	published by Kennedy et al., 2011, FSI	-2.15223	46
PC chu	29.7631	-95.3631	published by Kennedy et al., 2011, FSI	-2.19767	46
NT hom	32.7833	-96.8	published by Kennedy et al., 2011, FSI	0.038213	46
AT	30.2669	-97.7428	published by Kennedy et al., 2011, FSI	-2.64948	46

Site Name	Latitude	Longitude	Sample Comments	$\delta^{18}\text{O}$	Project ID
PC hom	29.7631	-95.3631	published by Kennedy et al., 2011, FSI	-1.50088	46
PC chu	29.7631	-95.3631	published by Kennedy et al., 2011, FSI	-1.60883	46
AT	30.2669	-97.7428	published by Kennedy et al., 2011, FSI	-2.46808	46
NT hom	32.7833	-96.8	published by Kennedy et al., 2011, FSI	0.476934	46
PC hom	29.7631	-95.3631	published by Kennedy et al., 2011, FSI	-1.37254	46
PC chu	29.7631	-95.3631	published by Kennedy et al., 2011, FSI	-1.3317	46
NT hom	32.7833	-96.8	published by Kennedy et al., 2011, FSI	0.681581	46
AT	30.2669	-97.7428	published by Kennedy et al., 2011, FSI	-2.47797	46
PC hom	29.7631	-95.3631	published by Kennedy et al., 2011, FSI	-1.02796	46

Site Name	Latitude	Longitude	Sample Comments	$\delta^{18}\text{O}$	Project ID
PC chu	29.7631	-95.3631	published by Kennedy et al., 2011, FSI	-1.25895	46
PC hom	29.7631	-95.3631	published by Kennedy et al., 2011, FSI	-1.03376	46
PC chu	29.7631	-95.3631	published by Kennedy et al., 2011, FSI	-1.03915	46
AT	30.2669	-97.7428	published by Kennedy et al., 2011, FSI	-1.8504	46
NT hom	32.7833	-96.8	published by Kennedy et al., 2011, FSI	1.157827	46
NT hom	32.7833	-96.8	published by Kennedy et al., 2011, FSI	1.067405	46
PC hom	29.7631	-95.3631	published by Kennedy et al., 2011, FSI	-4.47921	46
PC chu	29.7631	-95.3631	published by Kennedy et al., 2011, FSI	-3.68143	46
PC hom	29.7631	-95.3631	published by Kennedy et al., 2011, FSI	-1.24346	46

Site Name	Latitude	Longitude	Sample Comments	$\delta^{18}\text{O}$	Project ID
PC chu	29.7631	-95.3631	published by Kennedy et al., 2011, FSI	-0.59549	46
AT	30.2669	-97.7428	published by Kennedy et al., 2011, FSI	-1.33326	46
AT	30.2669	-97.7428	published by Kennedy et al., 2011, FSI	-0.90998	46
PC hom	29.7631	-95.3631	published by Kennedy et al., 2011, FSI	-1.01848	46
PC chu	29.7631	-95.3631	published by Kennedy et al., 2011, FSI	-0.95709	46
NT hom	32.7833	-96.8	published by Kennedy et al., 2011, FSI	1.15237	46
AT	30.2669	-97.7428	published by Kennedy et al., 2011, FSI	-0.83445	46
PC hom	29.7631	-95.3631	published by Kennedy et al., 2011, FSI	-1.19892	46
PC chu	29.7631	-95.3631	published by Kennedy et al., 2011, FSI	-0.77733	46

Site Name	Latitude	Longitude	Sample Comments	$\delta^{18}\text{O}$	Project ID
AT	30.2669	-97.7428	published by Kennedy et al., 2011, FSI	-1.37033	46
PC hom	29.7631	-95.3631	published by Kennedy et al., 2011, FSI	-0.95863	46
PC chu	29.7631	-95.3631	published by Kennedy et al., 2011, FSI	-0.89375	46
NT hom	32.7833	-96.8	published by Kennedy et al., 2011, FSI	-0.01705	46
AT	30.2669	-97.7428	published by Kennedy et al., 2011, FSI	-1.53401	46
PC hom	29.7631	-95.3631	published by Kennedy et al., 2011, FSI	-1.11152	46
PC chu	29.7631	-95.3631	published by Kennedy et al., 2011, FSI	-1.09734	46
NT hom	32.7833	-96.8	published by Kennedy et al., 2011, FSI	-0.17333	46
AT	30.2669	-97.7428	published by Kennedy et al., 2011, FSI	-1.18548	46

Site Name	Latitude	Longitude	Sample Comments	$\delta^{18}\text{O}$	Project ID
PC hom	29.7631	-95.3631	published by Kennedy et al., 2011, FSI	-1.0222	46
PC chu	29.7631	-95.3631	published by Kennedy et al., 2011, FSI	-0.92459	46
PC hom	29.7631	-95.3631	published by Kennedy et al., 2011, FSI	-2.44747	46
PC chu	29.7631	-95.3631	published by Kennedy et al., 2011, FSI	-2.23517	46
PC hom	29.7631	-95.3631	published by Kennedy et al., 2011, FSI	-2.5256	46
PC chu	29.7631	-95.3631	published by Kennedy et al., 2011, FSI	-2.24334	46
PC hom	29.7631	-95.3631	published by Kennedy et al., 2011, FSI	-0.90911	46
PC chu	29.7631	-95.3631	published by Kennedy et al., 2011, FSI	-0.49387	46
AT	30.2669	-97.7428	published by Kennedy et al., 2011, FSI	-1.03083	46

Site Name	Latitude	Longitude	Sample Comments	$\delta^{18}\text{O}$	Project ID
PC hom	29.7631	-95.3631	published by Kennedy et al., 2011, FSI	-1.2474	46
PC chu	29.7631	-95.3631	published by Kennedy et al., 2011, FSI	-1.12948	46
PC hom	29.7631	-95.3631	published by Kennedy et al., 2011, FSI	-3.57997	46
PC chu	29.7631	-95.3631	published by Kennedy et al., 2011, FSI	-3.87682	46
AT	30.2669	-97.7428	published by Kennedy et al., 2011, FSI	-0.60331	46
AT	30.2669	-97.7428	published by Kennedy et al., 2011, FSI	-0.94998	46
AT	30.2669	-97.7428	published by Kennedy et al., 2011, FSI	-0.09402	46
PC hom	29.7631	-95.3631	published by Kennedy et al., 2011, FSI	-2.72531	46
PC chu	29.7631	-95.3631	published by Kennedy et al., 2011, FSI	-2.52585	46

Site Name	Latitude	Longitude	Sample Comments	$\delta^{18}\text{O}$	Project ID
AT	30.2669	-97.7428	published by Kennedy et al., 2011, FSI	-0.27217	46
Abilene	32.4	-99.7	published by Bowen et al., 2007, WRR	3.166667	77
College Station	30.6	-96.3	published by Bowen et al., 2007, WRR	-1.44571	77
Wichita Falls	34	-98.5	published by Bowen et al., 2007, WRR	4.2	77
Dallas	32.8	-96.8	published by Bowen et al., 2007, WRR	-0.28586	77
Canyon	35	-101.9	published by Bowen et al., 2007, WRR	-3.46589	77
Edinburg	26.3	-98.2	published by Bowen et al., 2007, WRR	-1.89318	77
San Angelo	31.5	-100.4	published by Bowen et al., 2007, WRR	-3.75831	77
Lubbock	33.7	-101.8	published by Bowen et al., 2007, WRR	0.412896	77
El Paso	31.8	-106.5	published by Bowen et al., 2007, WRR	-9.92059	77
Alpine	30.4	-103.7	published by Bowen et al., 2007, WRR	-6.40156	77
Odessa	31.8	-102.4	published by Bowen et al., 2007, WRR	2.651826	77
San Angelo	31.5	-100.4	published by Bowen et al., 2007, WRR	1.721079	77
Waco	31.5	-97.1	published by Bowen et al., 2007, WRR	-2.84294	77

Site Name	Latitude	Longitude	Sample Comments	$\delta^{18}\text{O}$	Project ID
Dumas	35.9	-102	published by Bowen et al., 2007, WRR	-7.22	77
Corpus Christi	27.8	-97.4	published by Bowen et al., 2007, WRR	-4.03188	77
Fort Worth, TX	32.649	-97.358		-1.9	90
Wichita Falls, TX	33.883	-98.53		0.01	90
San Angelo, TX	31.429	-100.45		1.24	90
Conroe, TX	30.183	-95.449		-4.52	90
College Station, TX	30.623	-96.341		-4.88	90
San Antonio, TX	29.563	-98.594		-3.92	90
Corpus Christi, TX	27.717	-97.327		-1.87	90
Austin, TX	30.336	-97.663		-2.02	90
Lubbock, TX	33.585	-101.877		-4.21	90
El Paso, TX	31.75	-106.341		-8.29	90
Houston, TX	29.889	-95.575		-1.84	90
Corpus Christi, TX	27.717	-97.327		-1.86	90
Dallas, TX	32.785	-96.802		-1.87	90
Dallas, TX	32.785	-96.802		-1.93	90
Fort Worth, TX	32.649	-97.358		-1.055	90
Wichita Falls, TX	33.883	-98.53		0.95	90
San Angelo, TX	31.429	-100.45		0.86	90
Houston, TX	29.889	-95.575		-1.955	90
Conroe, TX	30.183	-95.449		-4.395	90
College Station, TX	30.623	-96.341		-4.685	90

<b>Site Name</b>	<b>Latitude</b>	<b>Longitude</b>	<b>Sample Comments</b>	<b><math>\delta^{18}\text{O}</math></b>	<b>Project ID</b>
San Antonio, TX	29.563	-98.594		-3.67	90
Corpus Christi, TX	27.717	-97.327		-1.885	90
Corpus Christi, TX	27.717	-97.327		-1.805	90
Austin, TX	30.336	-97.663		-2.085	90
Lubbock, TX	33.585	-101.877		-4.315	90
El Paso, TX	31.75	-106.341		-10.31	90

**APPENDIX C.** Modified data of query summarized in appendix B. Results conducted with identical project ID and coordinates are averaged.

Site Name	Latitude	Longitude	Sample Comments	$\delta^{18}\text{O}$	Project ID
Edinburg	26.3	-98.2	published by Bowen et al., 2007, WRR	-1.89318	77
	27.5013	-99.4369	Old ID: JB 01	-2.84299	275
Corpus Christi, TX	27.717	-97.327		-1.855	90
USATXCorpus Christi	27.73898	-97.4361	Old ID: 51721	-4.03188	275
Corpus Christi	27.8	-97.4	published by Bowen et al., 2007, WRR	-4.03188	77
Rio Grande Village Camp	29.18044	-102.956		-7.40727	3
K Bar Ranch House	29.30552	-103.178		-7.48743	3
Panther Junction	29.32773	-103.206		-7.32867	3
Hotel Contessa	29.4232	-98.4896		-4.2381	99
USATXSan Antonio	29.4239	-98.4933		-3.61097	275
SAT airport	29.52841	-98.4725		-4.33246	99
San Antonio, TX	29.563	-98.594		-3.795	90
USATXLuling	29.6494	-97.6494		-3.70901	275
USATXLuling	29.6818	-97.6494	Old ID: Water #38	-3.84515	275
Valero	29.69783	-95.2025		-2.45191	183
USATXColumbus	29.706	-96.5468		-4.3972	275
Kari_s parent_s house	29.75394	-95.7315		-4.79172	183
USATXHouston	29.76	-95.36	Old ID: 42453	-2.98709	275
USATXHouston	29.7631	-95.3631		-2.4516	275
PC chu	29.7631	-95.3631	published by Kennedy et al., 2011, FSI	-1.90766	46
Codys Bistro	29.8282	-97.9874	Restroom sink	-3.44085	225
Academy	29.84818	-97.9682	Restroom sink	-3.504	225
7-Eleven Gas Station	29.85583	-97.9528	Womens bathroom	-3.42081	225
Lower Purgatory Creek trailhead	29.86572	-97.9642	tallest water fountain	-3.4203	225
Burger King	29.86689	-97.9391	Mens bathroom sink	-3.37967	225

Site Name	Latitude	Longitude	Sample Comments	$\delta^{18}\text{O}$	Project ID
The Comfort Inn & Suites	29.8691	-97.9375		-3.41293	225
The Woods Apt Complex	29.87248	-97.9289		-3.3596	225
Pac N Sac Gas Station	29.87639	-97.9286		-3.43287	225
Englebrook Apartments	29.88208	-97.94	kitchen sink	-3.38159	225
Hobby Lobby	29.88306	-97.9172	Womens bathroom	-3.4359	225
Walmart	29.88325	-97.9137	Mens Restroom sink	-3.40262	225
San Marcos Activity Center	29.88472	-97.9322	Water fountains	-3.43498	225
Texas State University Greenhouse	29.88609	-97.9466	Restroom sink	-4.23794	225
Mochas and Javas in HEB	29.8873	-97.9263	restraunt sink	-3.40075	225
Sewell Park Outdoor Center	29.88732	-97.9337	Womens bathroom	-4.26454	225
Houston, TX	29.889	-95.575		-1.8975	90
Texas State University Comal Building	29.88934	-97.9409	Restroom sink	-4.253	225
San Marcos DMV	29.89025	-97.9137		-3.38507	225
Mochas and Javas	29.89194	-97.9397	Water fountains	-3.46056	225
Evans Liberal Arts Building on Texas State University Campus	29.89222	-97.9464	Womens bathroom	-4.22379	225
The Meadows Center for Water and the Environment	29.89389	-97.9294		-3.40085	225
Iconic Village Apartments 100 Building	29.89669	-97.9419	bathroom sink	-3.81215	225
Walgreens	29.89685	-97.9647		-3.67124	225
Texaco	29.89706	-97.9218	unisex bathroom	-3.45619	225
The Pita Shop	29.89863	-97.971	Womens bathroom	-3.87391	225
Sunco Gas Station	29.8997	-97.9078	Womens bathroom	-3.41997	225

Site Name	Latitude	Longitude	Sample Comments	$\delta^{18}\text{O}$	Project ID
The Grove Apartments	29.90194	-97.9025	kitchen sink	-3.42584	225
St. Marks Episcopal Church	29.9046	-97.9958	Restroom sink	-4.40978	225
Alpha Sigma Phi Fraternity House	29.9067	-98.0069	Sink	-4.24506	225
IAH airport	29.98574	-95.3361		-4.51163	99
USATXKerrville	30.0667	-99.1647		-4.69959	275
USATXKerrville	30.0667	-99.1632	Old ID: Water #36	-4.21848	275
T78 airport	30.08012	-94.6977		-4.6858	225
	30.0858	-94.1017	Old ID: Trip03_W3003	-3.44499	275
	30.093	-93.7366	Old ID: Orange tap	-4.45337	275
GYB airport	30.17055	-96.9791		-5.16069	225
Conroe, TX	30.183	-95.449		-4.4575	90
Steph_s house	30.19575	-97.7803		-1.18254	183
Airport Diner	30.24443	-98.908		-3.70702	225
Hampton	30.26409	-97.742		-2.83536	99
AT	30.2669	-97.7428		-1.9516	275
AT	30.2669	-97.7428	published by Kennedy et al., 2011, FSI	-2.25852	46
	30.2672	-97.7431	Old ID: Austin, TX tap	-1.63772	275
Austins Inn	30.2829	-97.7471		-1.89542	225
East Austin	30.3146	-97.6973		-2.90145	225
Austin, TX	30.336	-97.663		-2.0525	90
6R3 airport	30.35968	-95.0079		-4.44	225
60R airport	30.37377	-96.1146		-4.54902	225
Super 8 Motel	30.38356	-94.3167		-4.04266	183
EDC airport	30.39996	-97.5734		-2.15503	225
Alpine	30.4	-103.7	published by Bowen et al., 2007, WRR	-6.40156	77
	30.4894	-99.772	Old ID: Junction tap	-4.5276	275
JCT airport	30.51025	-99.7656		-4.75283	225
College Station	30.6	-96.3	published by Bowen et al., 2007, WRR	-1.44571	77
College Station, TX	30.623	-96.341		-4.7825	90

Site Name	Latitude	Longitude	Sample Comments	$\delta^{18}\text{O}$	Project ID
	30.628	-96.3344	Old ID: 2012 SIE 32	-5.06245	275
	30.711	-101.212	Old ID: Ozona tap	-4.57909	275
OZA airport	30.7313	-101.203		-5.60591	225
UTS airport	30.7429	-95.5861		-3.77712	225
	30.894	-102.879	Old ID: Fort Stockton tap	-7.84236	275
La Quinta	30.8986	-102.909		-7.92484	3
	31.0399	-104.831	Old ID: Guadalupe Mountains tap	-9.12453	275
Shell	31.05409	-97.4547		-1.26133	183
VHN airport	31.06086	-104.786		-7.81255	225
PEQ airport	31.39	-103.511		-6.98362	225
USATXPecos	31.4156	-103.49	Old ID: Water #24	-6.9133	275
USATXPecos	31.4198	-103.492	Old ID: Water #23	-6.85901	275
USATXSan Angelo	31.4198	-100.441	Old ID: Water #31	1.325974	275
USATXSan Angelo	31.4253	-100.495	Old ID: Water #33	1.610471	275
USATXSan Angelo	31.4255	-100.497	Old ID: Water #32	1.607285	275
USATXPecos	31.4263	-103.494	Old ID: Water #22	-6.95651	275
San Angelo, TX	31.429	-100.45		1.05	90
San Angelo	31.5	-100.4	published by Bowen et al., 2007, WRR	-0.10538	77
Waco	31.5	-97.1	published by Bowen et al., 2007, WRR	-2.84294	77
	31.5493	-97.1467	Old ID: 2012 SIE 03	-3.38429	275
Waco Mammoth NM Vistor Center	31.60677	-97.176		-0.96465	183
El Paso, TX	31.75	-106.341		-9.3	90
	31.7586	-106.486		-11.0581	
INK airport	31.7828	-103.196		-5.91293	225
Wyndham	31.79669	-106.398		-10.4143	225
El Paso	31.8	-106.5	published by Bowen et al., 2007, WRR	-9.92059	77
Odessa	31.8	-102.4	published by Bowen et al., 2007, WRR	2.651826	77

Site Name	Latitude	Longitude	Sample Comments	$\delta^{18}\text{O}$	Project ID
USATXOdessa	31.8423	-102.366	Old ID: Water #25	0.206524	275
USATXOdessa	31.8552	-103.375		0.41226	
Comfort Suites Odessa	31.89994	-102.337		-0.28599	3
Wildcatter Aviation	31.92276	-102.393		-0.27154	3
Exxon	31.94601	-94.2394		-5.01762	183
Shell	32.24359	-96.4971		0.16219	183
USATXBig Spring	32.25	-101.479		0.609761	275
Short St	32.34147	-97.4275		-1.17612	225
Valero	32.34697	-95.3165		-5.72276	183
Ray St	32.37788	-97.3322		-5.53572	225
Abilene	32.4	-99.7	published by Bowen et al., 2007, WRR	3.166667	77
Victory Forest	32.4158	-97.1948		-1.49834	225
QT gas station	32.46013	-96.8422		-1.30944	225
N Creek Circle	32.46954	-96.8118		-1.28812	225
Cheshire St	32.62557	-97.3436		-1.65602	225
Willow Springs	32.63944	-97.1718		-1.47495	225
Heahtherbrook Dr	32.64453	-97.1632		-1.51213	225
Fort Worth, TX	32.649	-97.358		-1.4775	90
Gas station	32.66159	-96.8917		-1.64113	225
Summit Ave	32.7327	-97.1213		-1.49409	225
Pinnacle Bank	32.7587	-97.1139		-1.63699	225
7-11 store	32.75906	-96.8205		-1.686	225
Shell	32.76097	-94.3553		-1.74997	183
NT hom	32.7833	-96.8		-1.42391	
NT hom	32.7833	-96.8	published by Kennedy et al., 2011, FSI	-0.16343	46
Dallas, TX	32.785	-96.802		-1.9	90
Jack in the Box	32.79195	-96.7506		-1.62576	225
Dallas	32.8	-96.8	published by Bowen et al., 2007, WRR	-0.28586	77
Stutz Dr	32.82205	-96.8386		-1.53091	225
	32.89667	-97.0381	Old ID: JB 03	0.172622	275
	32.897	-97.038	Old ID: Dallas-Fort Worth tap	-2.37845	275
Bay Meadows Dr	32.96677	-97.1298		-0.64694	225

Site Name	Latitude	Longitude	Sample Comments	$\delta^{18}\text{O}$	Project ID
McDonalds	32.98794	-96.8417		-1.4707	225
Moccasin Dr	33.06917	-96.7153		-1.89099	225
Lubbock, TX	33.585	-101.877		-4.2625	90
Lubbock	33.7	-101.8	published by Bowen et al., 2007, WRR	0.412896	77
Wichita Falls, TX	33.883	-98.53		0.48	90
Wichita Falls	34	-98.5	published by Bowen et al., 2007, WRR	4.2	77
Canyon	35	-101.9	published by Bowen et al., 2007, WRR	-3.46589	77
USATXArnot	35.18932	-102.011	Old ID: ANTTX0408	-6.94661	275
USATXAlanreed	35.2144	-100.74	Old ID: ALRTX0409	-5.7315	275
USATXAmarillo	35.2219	-101.831		-3.34043	275
Dumas	35.9	-102	published by Bowen et al., 2007, WRR	-7.22	77
USANMDalhart	36.0606	-102.348		-6.98689	275

**APPENDIX D.** Isotopic results obtained for vials 1-52. Vial IDs 6, 18, and 27 are bolded, highlighted, and italicized to indicate omission from analyses.

Vial ID	Latitude	Longitude	$\delta^{18}\text{O}_{\text{vsmow}} (\text{‰})$
1	30.1862	-97.7745	-1.2143143697
2	30.1876	-97.7644	-1.2411307272
3	30.2081	-97.7797	-1.1969458267
4	30.2375	-97.7397	-1.2108744312
5	30.2664	-97.7349	-1.1684680184
<b>6</b>	<b>30.2810</b>	<b>-97.6522</b>	<b>-0.9821811709</b>
7	30.3048	-97.6824	-0.9440820011
8	30.3051	-97.6971	-1.087124555
9	30.3770	-97.6593	-1.328512908
10	30.3957	-97.6368	-1.1553662141
11	30.4033	-97.6853	-0.4982110932
12	30.3645	-97.7163	-0.9761054238
13	30.3638	-97.7164	-1.1543490149
14	30.3318	-97.6863	-1.0781281334
15	30.3255	-97.7400	-1.1842697713
16	30.3260	-97.7400	-1.0878736452
17	30.2816	-97.7752	-1.1291668575
<b>18</b>	<b>30.2912</b>	<b>-97.7871</b>	<b>-1.1905307128</b>
19	30.2807	-97.8069	-1.1658487732
20	30.2572	-97.8075	-1.187606959
21	30.2283	-97.7889	-1.1186518763
22	30.1690	-97.7869	-1.1951474813
23	29.5927	-98.3512	-4.47326009
24	29.6108	-98.4690	-4.764416568
25	29.6159	-98.4935	-4.343423593
26	29.6159	-98.4935	-5.139233378
<b>27</b>	<b>29.5984</b>	<b>-98.4773</b>	<b>0.5338896597</b>
28	29.5946	-98.4577	-5.1165003089
29	29.5700	-98.5189	-5.0716468353
30	29.5403	-98.5532	-3.9718476550
31	29.5433	-98.5808	-4.0809080203
32	29.5162	-98.6234	-3.8816039315
33	29.4829	-98.6020	-3.3222537098
34	29.4322	-98.6569	-4.0338356059
35	29.4222	-98.6775	-3.7635974618

<b>Vial ID</b>	<b>Latitude</b>	<b>Longitude</b>	<b><math>\delta^{18}\text{O}_{\text{vSMOW}}</math> (‰)</b>
36	29.4320	-98.6266	-4.0123929928
37	29.3591	-98.5957	-4.4924751559
38	29.3065	-98.5613	-4.4352945362
39	29.3312	-98.4966	-4.4337261100
40	29.3643	-98.4593	-4.3902016990
41	29.3543	-98.4322	-4.4292180700
42	29.3682	-98.4372	-4.3919218803
43	29.4203	-98.4452	-4.2842267470
44	29.4189	-98.4878	-4.1638519870
45	29.4360	-98.5488	-4.0919009369
46	29.4901	-98.5193	-3.9822477301
47	29.4948	-98.4667	-3.9788634711
48	29.4761	-98.4607	-4.0079443061
49	29.5081	-98.4219	-4.6534270926
50	29.4844	-98.3713	-4.3475234849
51	29.5322	-98.3805	-3.9845083044
52	29.5548	-98.3469	-4.0315947031

**APPENDIX E.** Additional donors sampled and are to be added to analyses in future works.

<b>TXSTDSC Donor ID</b>
2015.042
2017.029
2018.033
2018.057
2019.007
2019.025
2019.030

## REFERENCES

- Bartelink, E. J., & Chesson, L. A. (2019). Recent applications of isotope analysis to forensic anthropology. *Forensic Sciences Research*, 4, 29-44.
- Bowen, G. J., Ehleringer, J. R., Chesson, L. A., Stange, E., & Cerling, T. E. (2007). Stable isotope ratios of tap water in the contiguous United States. *Water Resources Research*, 43, W03419.
- Bowen, G. J., & Revenaugh, J. (2003). Interpolating the isotopic composition of modern meteoric precipitation. *Water Resources Research*, 39, 1299.
- Centers for disease control and prevention (CDC, 2019). *Division of diabetes translation website*. Retrieved December 07, 2019, from <https://www.cdc.gov/diabetes/library/reports/reportcard/incidence-2017.html>
- Centers for Disease Control and Prevention (CDC, 2020a). *National diabetes statistics report*. Retrieved July 26, 2021, from <https://www.cdc.gov/diabetes/pdfs/data/statistics/national-diabetes-statistics-report.pdf>
- Centers for Disease Control and Prevention (CDC, 2020b). *Sickle Cell Disease (SCD)*. Retrieved July 26, 2021, from <https://www.cdc.gov/ncbddd/sicklecell/facts.html>
- Cerling, T. E., Wittemyer, G., Rasmussen, H. B., Vollrath, F., Cerling, C. E., Robinson, T. J., & Douglas-Hamilton, I. (2006). Stable isotopes in elephant hair document migration patterns and diet changes. *Proceedings of the National Academy of Sciences of the United States of America*, 103, 371-373.

- Chesson, L. A., Barnette, J. E., Bowen, G. J., ET AL. (2018). Applying the principles of isotope analysis in plant and animal ecology to forensic science in the Americas. *Oecologia*, 187, 1077-1094.
- Chesson, L. A., Valenzuela, L. O., O'Grady, S. P., Cerling, T. E., & Ehleringer, J. R. (2010). Links between purchase location and stable isotope ratios of bottled water, soda, and beer in the United States. *Journal of Agricultural and Food Chemistry*, 58, 7311-7316.
- Coplen, T. B., Landwehr, J. M., Qi, H., & Jennifer, M. L. (2013). The  $\delta^2\text{H}$  and  $\delta^{18}\text{O}$  of Tap Water from 349 Sites in the United States and Selected Territories. *U.S. Geological Survey Data Series 703*, 113 p., from <http://pubs.usgs.gov/ds/703>
- Craig, H. (1961). Isotopic variations in meteoric waters. *Science*, 133, 1702–1703.
- D'Angela, D., & Longinelli, A. (1990). Oxygen isotopes in living mammal's bone phosphate: Further results. *Chemical Geology*, 86, 75-82.
- Ehleringer, J. R., Bowen, G. J., Chesson, L. A., West, A. G., Podlesak, D. W., & Cerling, T. E. (2008). Hydrogen and oxygen isotope ratios in human hair are related to geography. *Proceedings of the National Academy of Sciences of the United States of America*, 105, 2788-2793.
- Epstein, S., & Zeiri, L. (1988). Oxygen and carbon isotopic compositions of gases respired by humans. *Proceedings of the National Academy of Sciences United States of America*, 85, 1727-1731.
- Fuller, B. T., Fuller, J. L., Sage, N. E., Harris, D. A., O'Connell, T. C., & Hedges, R. E. M. (2004). Nitrogen balance and  $\delta^{15}\text{N}$ : Why you're not what you eat during pregnancy. *Rapid Communications in Mass Spectrometry*, 18, 2889– 2896.

- Fuller, B. T., Fuller, J. L., Sage, N. E., Harris, D. A., O'Connell, T. C., & Hedges, R. E. M. (2005). Nitrogen balance and  $\delta^{15}\text{N}$ : Why you're not what you eat during nutritional stress. *Rapid Communications in Mass Spectrometry*, *19*, 2497–2506.
- Hatch, K. A., Crawford, M. A., Kunz, A. W., Thomsen, S. R., Eggett, D. L., Nelson, S. T., & Roeder, B. L. (2006). An objective means of diagnosing anorexia nervosa and bulimia nervosa using  $^{15}\text{N}/^{14}\text{N}$  and  $^{13}\text{C}/^{12}\text{C}$  ratios in hair. *Rapid Communications in Mass Spectroscopy*, *20*, 3367-3373.
- Hobson, K. A., Alisauskas, R. T., & Clark, R. G. (1993). Stable- nitrogen isotope enrichment in avian tissues due to fasting and nutritional stress: Implications for isotopic analyses of diet. *The Condor*, *95*, 388–394.
- Jaouen, K. & Pons, M. (2017). Potential of non-traditional isotope studies for bioarchaeology. *Archaeological and Anthropological Sciences*, *9*, 1389-1404.
- Katzenberg, A. M., Herring, D. A., Saunders, S. R. (1996). Weaning and infant mortality: evaluating the skeletal evidence. *Yearbook of Physical Anthropology*, *39*, 177-199.
- Katzenberg, M.A., & Lovell, N.C. (1999). Stable isotope variation in pathological bone. *International Journal of Osteoarchaeology*, *9*, 316-324.
- Kennedy, C. D., Bowen, G. J., & Ehleringer, J. R. (2011). Temporal variation of oxygen isotope ratios ( $\text{d}^{18}\text{O}$ ) in drinking water: Implications for specifying location of origin with human scalp hair. *Forensic Science International*, *208*, 156-166.
- Kohn, M. J. (1996). Predicting animal  $\delta^{18}\text{O}$ : Accounting for diet and physiological adaptation. *Geochimica et Cosmochimica Acta*, *60*, 4811.

- Krueger, H. W. & Sullivan, C. H. (1984). Models for carbon isotope fractionation between diet and bone. In Turnlund, J. R. & Johnson, P. E. (eds.), *Stable Isotopes in Nutrition* (pp. 205-220). American Chemical Society.
- Longinelli, A. (1984). Oxygen isotopes in mammal bone phosphate: A new tool for paleohydrological and paleoclimatological research? *Geochimica et Cosmochimica Acta*, 48, 385–390.
- Luz, B., Kolodny, Y., & Horowitz, M. (1984). Fractionation of oxygen isotopes between mammalian bone phosphate and environmental drinking water. *Geochimica et Cosmochimica Acta*, 48, 1689-1693.
- Madrigal, L. (2012). *Statistics for anthropology* (2nd ed.). Cambridge University Press.
- Nadal, A., Quesada, I., Tuduri, E., Nogueiras, R., & Alonso-Magdalena, P. (2017). Endocrine-disrupting chemicals and the regulation of energy balance. *Nature Reviews Endocrinology*, 13, 536-546.
- O’Grady, S. P., Wende, A. R., Remien, C. H., Valenzuela, L. O., Enright, L. E., Chesson, L. A., Abel, E. D., Cerling, T. E., & Ehleringer, J. R. (2010). Aberrant water homeostasis detected by stable isotope analysis, *PLoS ONE*, 5, 1-7.
- Olsen, K.C., White, C.D., Longstaffe, F.J., von Heyking, K., McGlynn, G., Grupe, G., & Rühli, F.J. (2014). Intraskelatal isotopic compositions ( $\delta^{13}\text{C}$ ,  $\delta^{15}\text{N}$ ) of bone collagen: Nonpathological and pathological variation. *American Journal of Physical Anthropology*, 153, 598-604.
- Petzke, K. J., Feist, T., Fleig, W. E., & Metges, C. C. (2006). Nitrogen isotopic composition in hair protein is different in liver cirrhotic patients. *Rapid Communications in Mass Spectrometry*, 20, 2973–2978.

- Podlesak, D. W., Bowen, G. J., O'Grady, S., Cerling, T. E., & Ehleringer, J. R. (2012).  $\delta^2\text{H}$  and  $\delta^{18}\text{O}$  of human body water: a GIS model to distinguish residents from non-residents in the contiguous USA. *Isotopes in Environmental and Health Studies*, 2, 259-279.
- Podlesak, D. W., Torregrossa, A. M., Ehleringer, J. R., Dearing, M. D., Passey, B. H., & Cerling, T. E. (2008). Turnover of oxygen and hydrogen isotopes in the body water,  $\text{CO}_2$ , hair, and enamel of a small mammal. *Geochimica et Cosmochimica Acta*, 72, 19-35.
- Reitsema, L.J. (2013). Beyond diet reconstruction: Stable isotope applications to human physiology, health, and nutrition. *American Journal of Human Biology*, 25, 445-456.
- Reitsema, L.J., & Crews, D.E. (2011). Brief communication: Oxygen isotopes as a biomarker for sickle-cell disease? Results from transgenic mice expressing human hemoglobin  $\beta$  genes. *American Journal of Physical Anthropology*, 145, 495-498.
- Richards, M., & Montgomery, J. (2012). Isotope analysis and paleopathology: A short review and future developments. In *The global history of paleopathology: Pioneers and prospects* (pp. 718-731). Oxford University Press.
- Schoeller, D. A. (1999). Isotope fractionation: Why aren't we what we eat? *Journal of Archaeological Science*, 26, 667-673.
- Schoeninger, M. J. (2011). Diet reconstruction and ecology using stable isotope ratios. In Larsen, C. S. (ed). *A companion to biological anthropology*. Chichester: Wiley-Blackwell.

- Schoeninger, M. J. & Katherine, M. (1992). Bone stable isotope studies in archaeology. *Journal of World Prehistory*, 6, 247– 296.
- Temple, D. H. (2018). Bioarchaeological evidence for adaptive plasticity and constraint: Exploring life-history trade-offs in the human past. *Evolutionary Anthropology*, 28, 34-46.
- Ubelaker, D. H. (2019). Forensic anthropology: Methodology and applications. In Katzenberg, M. A. & Grauer, A. L. (eds). *Biological anthropology of the human skeleton* (pp 43-71). John Wiley & Sons, Inc.
- United States Department of the Interior (DOI, 2014). *Texas State & County Boundaries 2014*. Retrieved June 22, 2021, from <https://data.tnris.org/collection/c439cfd8-4966-490f-9eea-eb2a8a11a3bd>
- United States Census Bureau. *QuickFacts Austin city, Texas; San Antonio city, Texas*. Retrieved July 11, 2021, from <https://www.census.gov/quickfacts/fact/table/austincitytexas,sanantoniocitytexas/PST045219>
- Warner, M. M., Plemons, A. M., Herrmann, N. P., & Regan, L. A. (2018). Refining stable oxygen and hydrogen isoscapes for the identification of human remains in Mississippi. *Journal of Forensic Sciences*, 63, 395-402.
- West, J. B., Sobek, A., & Ehleringer, J. R. (2008). A simplified GIS approach to modeling global leaf water isoscapes. *PLoS One*, 3, e2447.
- Widory, D. (2004). Oxygen and nitrogen isotopic fractionations during human respiration. *Comptes Rendus Biologies*, 153, 11-18.

Wood, J. W., Milner, G. R., Harpending, H. C., & Weiss, K. M. (1992). The osteological paradox: Problems of inferring prehistoric health from skeletal samples. *Current Anthropology*, 33, 343-370.